

Gaussian Process Regression with Location Errors

Daniel Cervone[†] and Natesh S. Pillai[†]

Harvard University[†]

Abstract. In this paper, we investigate Gaussian process regression models where inputs are subject to measurement error. In spatial statistics, input measurement errors occur when the geographical locations of observed data are not known exactly. Such sources of error are not special cases of “nugget” or microscale variation, and require alternative methods for both interpolation and parameter estimation. Gaussian process models do not straightforwardly extend to incorporate input measurement error, and simply ignoring noise in the input space can lead to poor performance for both prediction and parameter inference. We review and extend existing theory on prediction and estimation in the presence of location errors, and show that ignoring location errors may lead to Kriging that is not “self-efficient”. We also introduce a Markov Chain Monte Carlo (MCMC) approach using the Hybrid Monte Carlo algorithm that obtains optimal (minimum MSE) predictions, and discuss situations that lead to multimodality of the target distribution and/or poor chain mixing. Through simulation study and analysis of global air temperature data, we show that appropriate methods for incorporating location measurement error are essential to valid inference in this regime.

Key words and phrases: Gaussian processes, measurement error, Kriging, MCMC, geostatistics.

1. INTRODUCTION

Gaussian process models assume an output variable of interest varies smoothly over an input space (*e.g.*, precipitation totals across geographical coordinates, crop yield across factor levels of an experimental design). Such models appear frequently in areas as diverse as climate science [Mardia and Goodall (1993)], epidemiology [Lawson (1994)], and black-box problems such as computer experiments, and Bayesian optimization [Sacks et al. (1989), Srinivas et al. (2009)]. See Stein (1999), Cressie and Cassie (1993), Banerjee, Carlin and Gelfand (2014) and Gelman et al. (2014) for more detailed treatments.

Noisy spatial input data are common in many applications; for example, geostatistical data is often imprecisely spatially referenced, “binned” to the nearest

Department of Statistics, Harvard University, Cambridge, MA, USA (e-mail: dcervone@fas.harvard.edu; pillai@stat.harvard.edu).

[†]NSP was partially supported by an ONR grant. DC was partially supported by a research grant from the Harvard University Center for the Environment.

latitude/longitude grid point, or referenced to maps with distorted coordinates [Veregin (1999), Barber, Gelfand and Silander (2006)]. Accounting for measurement error on covariates in the context of regression models is a well studied theme [Carroll et al. (2006)]; however, despite their importance in applications, surprisingly little work has been done on interpolation or Gaussian process regression problems in the presence of (spatial) location measurement error. As we show in this paper, Gaussian process models do not straightforwardly extend to incorporate input measurement error, and simply ignoring noise in the input space can lead to poor performance.

Previous research on such error sources has mostly focused on demonstrating their existence and quantifying their magnitude [Bonner et al. (2003), Ward et al. (2005)]. For regression problems, Gabrosek and Cressie (2002) (and later Cressie and Kornak (2003)) adjust Kriging equations for the presence of location errors, and Fanshawe and Diggle (2011) further develop research for this regime to include problems where the locations of future observations or predictions are subject to error. Location errors have also been studied in the context of point process data [Zimmerman and Sun (2006), Zimmerman, Li and Fang (2010)].

Properly accounting for location errors is essential for optimal interpolation and uncertainty quantification, as well precise and efficient parameter estimation when parameters of the covariance function are unknown. Using theoretical results and extensive simulations, our paper provides guidelines on situations when location errors are most impactful for data analysis, and suggestions for incorporating this source of error into inference and prediction. We expand the research in Cressie and Kornak (2003) on best linear unbiased prediction (Kriging) to include procedures for obtaining interval forecasts and for quantifying the cost of ignoring location errors. We also discuss Markov Chain Monte Carlo (MCMC) methods for optimal (minimum mean squared error (MSE)) predictions, which average over the conditional distribution of (latent) location errors given the observed data.

Section 2 establishes notation and describes the basic model with location errors used throughout the paper. In Section 3, we discuss Kriging using the covariance structure of the location-error induced process. Section 4 considers MCMC methods for obtaining minimum MSE predictions, and thus improving upon Kriging. We compare these methods through simulation study in Section 5, and explore an application to interpolating northern hemisphere temperature anomalies in Section 6. The proofs of all of the theoretical results are given in an Appendix.

2. THE MODEL

We will write $\mathbf{s}_n = (s_1 \ s_2 \ \dots \ s_n)'$ to denote a n -vector of locations in the input space $\mathbb{S} \subset \mathbb{R}^p$, and $\mathbf{x}_n = (x(s_1) \ x(s_2) \ \dots \ x(s_n))'$ as the associated vector of observations at \mathbf{s}_n . Similarly, we will denote $\mathbf{x}_k^* = (x(s_1^*) \ \dots \ x(s_k^*))'$, or simply $x^* = x(s^*)$ where $\{s_i^*, i = 1, \dots, k\}$ are unobserved locations. The process $x : \mathbb{S} \rightarrow \mathbb{R}$ is called a *Gaussian process* if, for any $s_1, \dots, s_n \in \mathbb{S}$, $\mathbf{x}_n = (x(s_1)x(s_2) \ \dots \ x(s_n))'$ is jointly Normally distributed. Typically, the form of this joint distribution is specified by a deterministic or parametric mean function (for now, taken without

loss of generality to be 0) and a covariance function $c : \mathbb{S}^2 \rightarrow \mathbb{R}$, so that

$$(1) \quad \begin{pmatrix} x(s_1) \\ \vdots \\ x(s_n) \end{pmatrix} \sim \mathcal{N} \left(\mathbf{0}, \begin{pmatrix} c(s_1, s_1) & \cdots & c(s_1, s_n) \\ \vdots & \ddots & \\ c(s_n, s_1) & & c(s_n, s_n) \end{pmatrix} \right).$$

For c to be a valid covariance function, the covariance matrix in Equation (1) must be positive semi-definite for all input vectors $\mathbf{s}_n = (s_1 \ s_2 \ \dots \ s_n)'$.

Gaussian process regression is primarily used as a method for interpolating (predicting) values \mathbf{x}_k^* at unobserved points $\mathbf{s}_k^* = (s_1^* \ \dots \ s_k^*)'$ in the input space, given all available observations. Such conditional distributions are easily obtained by exploiting the joint normality of the response x at observed and unobserved locations:

$$(2) \quad \mathbf{x}_k^* | \mathbf{x}_n \sim \mathcal{N}(\mathbf{C}(\mathbf{s}_k^*, \mathbf{s}_n) \mathbf{C}(\mathbf{s}_n, \mathbf{s}_n)^{-1} \mathbf{x}_n, \mathbf{C}(\mathbf{s}_k^*, \mathbf{s}_k^*) - \mathbf{C}(\mathbf{s}_k^*, \mathbf{s}_n) \mathbf{C}(\mathbf{s}_n, \mathbf{s}_n)^{-1} \mathbf{C}(\mathbf{s}_n, \mathbf{s}_k^*)).$$

In Equation (2), $\mathbf{C}(\mathbf{s}_n, \mathbf{s}_n)$ denotes the covariance matrix of \mathbf{x}_n , $\mathbf{C}(\mathbf{s}_k^*, \mathbf{s}_n)$ denotes the $k \times n$ covariance matrix between \mathbf{x}_k^* and \mathbf{x}_n .

When the locations in the input space \mathbb{S} are affected by error, we observe a surrogate process $y : \mathbb{S} \rightarrow \mathbb{R}$,

$$y(s_i) = x(s_i + u_i),$$

where s_i is a known location in \mathbb{S} and $u_i \in \mathbb{S}$ is unobserved location error. The problem of Gaussian process regression with location errors addressed in this paper is to predict x at unobserved (exact) locations $x(s^*)$ given observations from the noise-corrupted process y .

When x is assumed to be a Gaussian process, there is no nontrivial structure for u that results in y being a Gaussian process. Additionally, it is not possible to write y as a convolution of x and a white noise process as differences between the surfaces y and x will generally be correlated across space, *i.e.*, $\text{Cov}[y(s_1) - x(s_1), y(s_2) - x(s_2)] \neq 0$. Gaussian process regression with location errors therefore cannot be thought of as a classical or Berkson errors-in-variables problem [Carroll et al. (2006)]. Interestingly, in some cases, the process y may be more informative for prediction at a new location $x(s^*)$ than the process x is. Thus, appropriate methods can deliver lower MSE interpolations in a location-error regime than the MSE of the usual methods in an error-free regime.

3. KRIGING THE LOCATION ERROR INDUCED PROCESS Y

As shown in Cressie and Kornak (2003), the second moment properties of y can be used to perform Kriging (they named this ‘‘Kriging adjusting for location error’’ or KALE), noting that measurement errors u induce a new covariance function

$$(3) \quad \begin{aligned} k(s_1, s_2) &= \text{Cov}[y(s_1), y(s_2)] = \mathbb{E}[c(s_1 + u_1, s_2 + u_2)] \text{ for } s_1 \neq s_2 \\ k(s, s) &= \mathbb{V}[y(s)] = \mathbb{E}[c(s + u, s + u)] \\ k^*(s, s^*) &= \text{Cov}[y(s), x(s^*)] = \mathbb{E}[c(s + u, s^*)]. \end{aligned}$$

The expectation here is taken over the input errors u , which are assumed to have some joint distribution $g_{\mathbf{s}_n}$. The following result shows that if c is a valid covariance function, then so is k , regardless of the error distribution $g(\cdot)$.

PROPOSITION 3.1. *Assume for all n and $\mathbf{s}_n \in \mathbb{S}$, $(u_1, u_2, \dots, u_n) \sim g_{\mathbf{s}_n} \in \mathcal{G}$, where \mathcal{G} is any family of probability measures on \mathbb{S} . Then k is a valid covariance function if c is.*

Regardless of the form of c , k always exhibits the “nugget” effect, or discontinuities in the covariance function [Matheron (1962)] $\lim_{s_2 \rightarrow s_1} k(s_2, s_1) \neq k(s_1, s_1)$. In fact, several authors cite location/positional error as a justification for including a nugget term in an arbitrary covariance function c [Cressie and Cassie (1993), Stein (1999)], alongside independent measurement error in observing the response, $x(s) + \epsilon$. Location errors, however, cause k to differ from c throughout the spatial domain \mathbb{S}^2 (this is shown in Figure 1), meaning that while they induce a nugget, a nugget term alone cannot capture the effect of location errors.

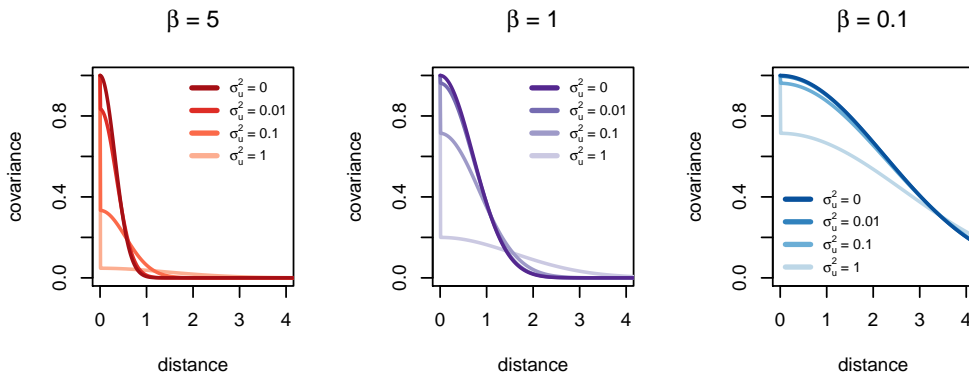


FIG 1. Comparison of c and k for $\mathbb{S} = \mathbb{R}^2$ and $c(s_1, s_2) = \exp(-\beta\|s_1 - s_2\|^2)$, with $u_i \stackrel{iid}{\sim} \mathcal{N}(0, \sigma_u^2 \mathbf{I}_2)$. Location errors $\sigma_u^2 > 0$ cause c and k to differ as a function of distance, and induce a nugget discontinuity at 0.

Using k , we get the Kriging estimator adjusting for location error for $x(s^*)$ at an unobserved location of x :

$$(4) \quad \hat{x}_{\text{KALE}}(s^*) = \mathbf{K}^*(s^*, \mathbf{s}_n) \mathbf{K}(\mathbf{s}_n, \mathbf{s}_n)^{-1} \mathbf{y}_n.$$

In Equation (4), \mathbf{K} and \mathbf{K}^* respectively denote the covariance matrices corresponding to the kernels k and k^* . The quantity $\hat{x}_{\text{KALE}}(s^*)$ is the best linear unbiased predictor for $x(s^*)$ (in terms of MSE) and has all the usual Kriging properties. When there are no location errors, the Kriging estimator is equivalent to the conditional expectation of $x(s^*)$ given \mathbf{x}_n (see Equation (2)).

In general, the covariance functions k and k^* can be evaluated using Monte Carlo integration by repeatedly sampling \mathbf{u}_n from g . For several common combinations of covariance function and location error models, however, it is possible to arrive at the expressions in Equation (3) in closed form. In particular, if

$$c(s_1, s_2) = \tau^2 \exp(-\beta d(s_1, s_2)),$$

then we can define a random variable $Z = d(s_1 + u_1, s_2 + u_2)$ and find its moment generating function $M_Z(t)$. If we can evaluate $M_Z(t)$ at $t = -\beta$, then this yields $k(s_1, s_2)$. For instance, for the squared exponential covariance function $d(s_1, s_2) = \|s_1 - s_2\|^2$ and Normal location errors $u \sim \mathcal{N}(0, \sigma_u^2 \mathbf{I}_p)$, Z has a scaled noncentral χ_p^2 distribution and

$$(5) \quad \begin{aligned} k(s_1, s_2) &= \frac{\tau^2}{(1 + 4\beta\sigma_u^2)^{p/2}} \exp\left(-\frac{\beta}{1 + 4\beta\sigma_u^2} \|s_1 - s_2\|^2\right) \text{ for } s_1 \neq s_2 \\ k(s, s) &= \tau^2 \end{aligned}$$

with a similar expression for $k^*(s, s^*)$. Thus the covariance function for y is also squared exponential (it is not generally true that c and k will share the same functional form). Note, however, that not all parameters are identifiable—we must know at least one of $(\tau^2, \beta, \sigma_u^2)$ in order to estimate the others.

Interestingly, it is possible for the KALE to yield lower MSE predictions than those given from an error-free regime, where $\mathbf{u}_n \equiv 0$ and $x = y$. In other words, \mathbf{y}_n can be more informative than \mathbf{x}_n for predicting $x(s^*)$. Heuristically, this happens when \mathbf{y}_n is more strongly correlated with $x(s^*)$ than is \mathbf{x}_n . Below we characterize the conditions for observing this phenomenon in a simple model with one observed data point (Figure 1 provides an illustration); it seems difficult to generalize this to larger observed location samples and covariance/error structures.

PROPOSITION 3.2. *Assume $n = 1$, $\|s - s^*\|^2 = \Delta^2$, $c(s, s^*) = \tau^2 \exp(-\beta\Delta^2)$ for all $s, s^* \in \mathbb{S}$, and $u \sim \mathcal{N}(0, \sigma_u^2 \mathbf{I}_p)$. Without location error ($\sigma_u^2 = 0$), the MSE in predicting $x(s^*)$ from $x(s)$ is $c_0 = \tau^2(1 - \exp(-2\beta\Delta^2))$. There exists $\sigma_u > 0$ such that $\mathbb{E}[(\hat{x}_{\text{KALE}}(s^*) - x(s^*))^2] < c_0$ if and only if $\beta\Delta^2 > p/2$.*

3.1 Interval predictions

For many applications of Gaussian process regression, particularly in geostatistics and environmental modeling, both point and interval predictions are of interest. However, Kriging, being strictly a moment-based procedure, does not provide uncertainty quantification for predictions other than variance. In a location-error Gaussian process regime, KALE predictions will always be non-Gaussian, thus variance alone is not sufficient to provide distributional or interval predictions.

However, it is relatively straightforward to derive confidence intervals for predictions at unobserved locations $x(s^*)$ given measurements \mathbf{y}_n at locations \mathbf{s}_n . The following proposition provides the exact distribution function (CDF) for prediction errors $x(s^*) - \hat{x}_{\text{KALE}}(s^*)$, which can be inverted to obtain a confidence interval for $x(s^*)$ based on $\hat{x}_{\text{KALE}}(s^*)$.

PROPOSITION 3.3. *Let*

$$\begin{aligned} V(\mathbf{u}_n) &= \sigma^2 + \gamma' \mathbf{C}(\mathbf{s}_n + \mathbf{u}_n, \mathbf{s}_n + \mathbf{u}_n) \gamma - 2\gamma' \mathbf{C}(\mathbf{s}_n + \mathbf{u}_n, s^*) \\ \text{where } \gamma &= \mathbf{K}(\mathbf{s}_n, \mathbf{s}_n)^{-1} \mathbf{K}^*(\mathbf{s}_n, s^*), \sigma^2 = \mathbb{V}[x(s^*)]. \end{aligned}$$

Then

$$(6) \quad \mathbb{P}(x(s^*) - \hat{x}_{\text{KALE}}(s^*) < z) = \mathbb{E} \left[\Phi \left(\frac{z}{\sqrt{V(\mathbf{u}_n)}} \right) \right],$$

where Φ is the CDF of the standard Normal distribution.

It may be necessary to evaluate Equation (6) using Monte Carlo; if so, it is practical to use the same draws of \mathbf{u}_n when evaluating different quantiles z , as this guarantees a Monte Carlo estimate of the distribution function be non-decreasing.

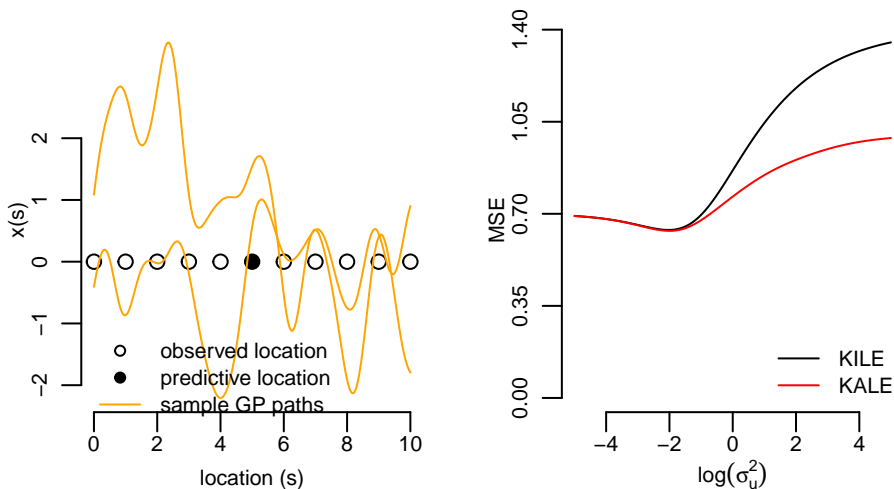
While intervals based on (6) provide exact coverage (modulo Monte Carlo error), such coverage is achieved by averaging over all data, both observed (\mathbf{y}_n) and unobserved ($x(s^*)$) as well as the location errors, \mathbf{u}_n . This is in contrast to usual interval estimates from Gaussian process regression without location error, which are exact probability statements conditional on the observed data \mathbf{x}_n . The reason this is an important distinction is because the usual Gaussian process conditional probability intervals yield the proper coverage rate across multiple prediction intervals (when predicting x at a collection of unobserved locations \mathbf{s}_k^*), whereas the confidence intervals corresponding to KALE may not.

3.2 Advantages over Kriging while Ignoring Location Errors

Failing to adjust for location errors when Kriging (Cressie and Kornak (2003) called this “Kriging ignoring location errors” or KILE) can lead to poor performance. A data analyst ignoring the location errors will use (see Equation (2))

$$(7) \quad \hat{x}_{\text{KILE}}(s^*) = \mathbf{C}(s^*, \mathbf{s}_n) \mathbf{C}(\mathbf{s}_n, \mathbf{s}_n)^{-1} \mathbf{y}_n.$$

Since $\hat{x}_{\text{KALE}}(s^*)$ is the best linear unbiased estimator for $x(s^*)$ and \hat{x}_{KILE} is also an unbiased linear estimator, KALE dominates KILE and always yields a reduced MSE. Figure 2 illustrates the disparity in MSE for a simple model; intuitively, the relative cost of ignoring location errors increases as the magnitude of the location errors increases. We also see in panel (B), illustrating Proposition 3.2, that for small values of σ_u^2 , the MSE for both KALE and KILE decreases in σ_u^2 .



(A) Locations at which we observe $y(s)$, as well as the location at which we wish to predict $x(s)$. Sample paths of Gaussian processes with this covariance function are also shown.

(B) For both KALE and KILE, MSE actually decreases as the magnitude of location errors increases when this magnitude is small. Above a certain point, greater location error yields higher MSE and greater disparity between KALE and KILE.

FIG 2. Here we assume $x(s)$ is a Gaussian process with mean 0 and covariance function $c(s_1, s_2) = \exp(-(s_1 - s_2)^2)$, with $u_i \stackrel{iid}{\sim} \mathcal{N}(0, \sigma_u^2)$. We compare MSE for predicting $x(5)$ based on $y(0), \dots, y(4)$ using KALE and KILE.

Besides yielding suboptimal predictions relative to KALE, ignoring location errors also leads to an estimator for $x(s^*)$ that is not self-efficient [p. 549, Meng (1994)]. Following Meng (1994), an estimator T for parameter θ is self-efficient if for any $\lambda \in [0, 1]$ and subset of the observed data $X_c \subset X$, we have

$$\mathbb{E}[(\lambda T(X) + (1 - \lambda)T(X_c) - \theta)^2] \geq \mathbb{E}[(T(X) - \theta)^2].$$

Thus, roughly speaking, self-efficient estimators are those that cannot be improved by using only a subset of the original data [Meng and Xie (2014)].

The following theorem states that the KILE MSE is unbounded as a function of any single spatial location s_i for $i = 1, \dots, n$. This is a stronger result than just the lack of self-efficiency. A consequence of Theorem 3.4 is that, assuming only simple continuity conditions on the covariance function and location error model, the KILE MSE can always increase when observing more data, regardless of the locations of the existing observations or the locations at which we want to make predictions.

THEOREM 3.4. *Suppose that the following conditions hold:*

- c is continuous and bounded in \mathbb{S}^2 ,
- the location error model g satisfies $(u_1^m, u_2^m) \xrightarrow{D} (u_1, u_2)$ for all $s_1, s_2 \in \mathbb{S}$ and sequences (s_1^m, s_2^m) such that $\lim_{m \rightarrow \infty} (s_1^m, s_2^m) = (s_1, s_2)$,
- and $\mathbb{P}(u_1 \neq u_2) < 1$ for all $s_1, s_2 \in \mathbb{S}$.

Let $\hat{x}_{\text{KILE}}(s^*)$ be the KILE estimator for $x(s^*)$ given \mathbf{y}_n . Then for any $M > 0$, $n \geq 2$, and $s_2, \dots, s_n \in \mathbb{S}$, there exists s_1 such that $\mathbb{E}[(x(s^*) - \hat{x}_{\text{KILE}}(s^*))^2] > M$.

Note that the condition that c is continuous excludes a nugget term from the distribution of x . We prove Theorem 3.4 (in the Appendix) by showing that when observed locations are very close together, the corresponding covariance matrix is nearly singular, and this increases MSE. Without location errors, the usual Kriging estimator does not exhibit this behavior since the difference between values of $x(s)$ for points that are close together also converges in probability to 0. This is not the case for the noise-corrupted process, as $y(s_2) - y(s_1)$ does not converge to 0.

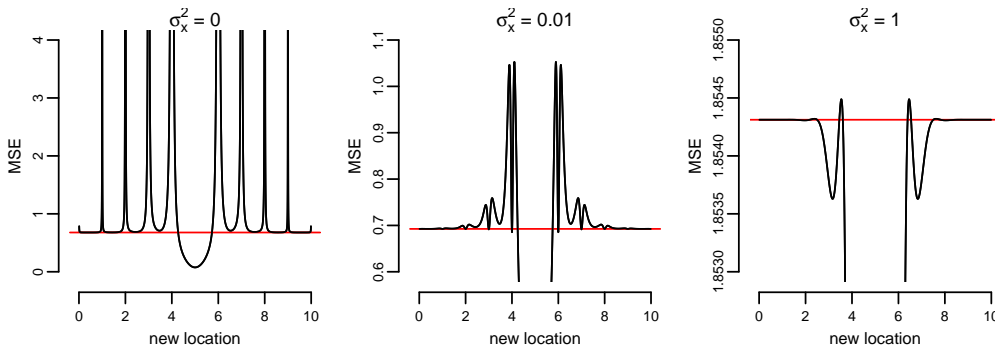


FIG 3. Here we assume $x(s)$ is a Gaussian process with mean 0 and covariance function $c(s, s^*) = \exp(-(s - s^*)^2) + \sigma_x^2 \mathbf{1}_{s=s^*}$. Location errors have the form $u_i \sim \mathcal{N}(0, 0.04)$. We use KILE to predict $x(5)$ based on $\mathbf{y}_{\text{obs}} = \{y(0), \dots, y(4), y(6), \dots, y(10)\}$, as well as an additional observation $y(s)$. The MSE in predicting $x(5)$ given \mathbf{y}_{obs} and $y(s)$ is plotted as a function of s , while the red line denotes the MSE based only on \mathbf{y}_{obs} . Despite the magnitude of the location errors being relatively small, observing another measurement of y at some locations can increase (possibly dramatically) the MSE.

Simulation results suggest that even when c contains a nugget term σ_x^2 , KILE is still not self-efficient, and additional observations can increase MSE. Figure 3 illustrates the change in MSE as a function of the location of an additional observation of y . Following Theorem 3.4, we see the MSE is unbounded when $\sigma_x^2 = 0$. But even when $\sigma_x^2 = 1$, it is possible for an additional observation to (slightly) increase MSE.

3.3 Parameter Estimation for Kriging

In typical applied settings, some or all parameters of the covariance function are unknown and must be estimated by the analyst in order to obtain Kriging equations. For Gaussian process models without a location error component, parameter estimation can be accomplished using likelihood methods. This can be computationally challenging for large data sets, as each likelihood evaluation requires a Cholesky factorization of the covariance matrix (or equivalent operations), which is $\mathcal{O}(n^3)$ except in special cases. An alternative is to choose parameters by maximizing goodness of fit between the empirical variogram and the theoretical (parametric) variogram, though this is less efficient for parametric Gaussian models.

Location errors present challenges for both such procedures as the covariance function for the observed process y (3) may not be available in closed form, meaning neither the likelihood function or variogram can be evaluated exactly. While Monte Carlo methods surely offer effective approaches in theory [Fanshawe and Diggle (2011)], they multiply the computational expense of the problem, as each evaluation of the likelihood requires M matrix factorizations, where M is the number of Monte Carlo samples used to approximate the likelihood. Cressie and Kornak (2003) advocate a pseudo-likelihood procedure [Carroll et al. (2006)] that uses a Gaussian likelihood approximation based on the first two moments of y ,

$$(8) \quad \tilde{L}(\theta; \mathbf{y}_n) \propto |\mathbf{K}_\theta(\mathbf{s}_n, \mathbf{s}_n)|^{-1/2} \exp\left(-\frac{1}{2}\mathbf{y}_n' \mathbf{K}_\theta(\mathbf{s}_n, \mathbf{s}_n)^{-1} \mathbf{y}_n\right),$$

where we write \mathbf{K}_θ to explicitly mark the dependence of the covariance function k on unknown parameters θ . This pseudo-likelihood requires inverting \mathbf{K} only once per pseudo-likelihood evaluation, even when \mathbf{K}_θ is computed by Monte Carlo.

We can work out inferential properties of the maximum pseudo-likelihood estimator $\hat{\theta} = \operatorname{argmax}_\theta \tilde{L}(\theta; \mathbf{y}_n)$. First, it is straightforward to check that the pseudo-score pertains to an unbiased estimating equation:

$$(9) \quad \mathbb{E}[\tilde{S}(\theta; \mathbf{y}_n)] = \mathbb{E}[\nabla \log(\tilde{L}(\theta; \mathbf{y}_n))] = \mathbf{0}.$$

Moreover, one can show the covariance matrix of the pseudo-score is given by

$$(10) \quad \begin{aligned} \tilde{G}(\theta) &= \mathbb{E}[\tilde{S}(\theta; \mathbf{y}_n) \tilde{S}(\theta; \mathbf{y}_n)'] \\ \tilde{G}(\theta)_{ij} &= \mathbb{E} \left[\frac{1}{2} \operatorname{Tr} \{ \Omega_i \mathbf{C}_\theta(\mathbf{u}_n) \Omega_j \mathbf{C}_\theta(\mathbf{u}_n) \} \right] \\ &+ \frac{1}{4} \left(\mathbb{E}[\operatorname{Tr} \{ \Omega_i \mathbf{C}_\theta(\mathbf{u}_n) \}] \operatorname{Tr} \{ \Omega_j \mathbf{C}_\theta(\mathbf{u}_n) \} \right) - \operatorname{Tr} \{ \Omega_i \mathbf{K}_\theta \} \operatorname{Tr} \{ \Omega_j \mathbf{K}_\theta \} \end{aligned}$$

using the notational abbreviations $\mathbf{C}_\theta(\mathbf{u}_n) = \mathbf{C}_\theta(\mathbf{s}_n + \mathbf{u}_n, \mathbf{s}_n + \mathbf{u}_n)$, $\mathbf{K}_\theta = \mathbf{K}_\theta(\mathbf{s}_n, \mathbf{s}_n) = \mathbb{E}[\mathbf{C}_\theta(\mathbf{u}_n)]$, and $\Omega_i = \mathbf{K}_\theta^{-1} \left(\frac{\partial}{\partial \theta_i} \mathbf{K}_\theta \right) \mathbf{K}_\theta^{-1}$. Lastly, the expected negative Hessian of the log pseudo-likelihood is

$$\begin{aligned} \tilde{H}(\theta)_{ij} &= \mathbb{E} \left[-\frac{\partial^2}{\partial \theta_i \partial \theta_j} \log(\tilde{L}(\theta; \mathbf{y}_n)) \right] \\ (11) \qquad &= \frac{1}{2} \text{Tr} \{ \Omega_i \mathbf{K}_\theta \Omega_j \mathbf{K}_\theta \}. \end{aligned}$$

If there are no location errors ($\mathbf{u}_n \equiv \mathbf{0}$), \tilde{L} is an exact likelihood and the second term in the right hand side of Equation (10) vanishes so that $\tilde{G}(\theta) = \tilde{H}(\theta)$, confirming the second Bartlett identity [Ferguson (1996)]. For non-zero location errors, however, we construct the Godambe information matrix as an analog to the Fisher information matrix [Varin, Reid and Firth (2011)],

$$\tilde{I}(\theta) = \tilde{H}(\theta) [\tilde{G}(\theta)]^{-1} \tilde{H}(\theta).$$

Evaluating $\tilde{I}(\theta)$ for different location error models illustrates the information loss in estimating covariance function parameters θ relative to the error-free case, where $\tilde{I}(\theta) = \tilde{G}(\theta) = \tilde{H}(\theta)$ is equivalent to the Fisher information matrix.

General theory of unbiased estimation equations [Heyde (1997)] suggests the asymptotic behavior of the pseudo-likelihood procedure satisfies

$$(12) \qquad \tilde{I}(\theta)^{1/2} (\hat{\theta} - \theta) \xrightarrow{D} \mathcal{N}(\mathbf{0}, \mathbf{I}).$$

However, Expression (12) does not hold in general even in an error-free regime $\mathbf{u}_n \equiv \mathbf{0}$, as asymptotic results for Gaussian process covariance parameters depend on the spatial sampling scheme used and the specific form of the covariance function [Stein (1999)]. We nevertheless expect (12) to hold for suitably well-behaved processes under increasing-domain asymptotics. Guyon (1982) gives an applicable result when locations \mathbf{s}_n are on a lattice. We are not aware of other theoretical results in this context.

4. MARKOV CHAIN MONTE CARLO METHODS

Markov Chain Monte Carlo methods offer an alternative to Kriging for prediction in a regime with noisy inputs. They allow us to compute the MSE-optimal prediction

$$\begin{aligned} \hat{x}(s^*) &= \mathbb{E}[x(s^*) | \mathbf{y}_n] \\ (13) \qquad &= \int (\mathbf{C}(s^*, \mathbf{s}_n + \mathbf{u}_n) [\mathbf{C}(\mathbf{s}_n + \mathbf{u}_n, \mathbf{s}_n + \mathbf{u}_n)]^{-1} \mathbf{y}_n) \pi(\mathbf{u}_n | \mathbf{y}_n) d\mathbf{u}_n, \end{aligned}$$

which will dominate the KALE estimator (4) in terms of MSE for any model and set of observed and predicted locations. The optimality of $\hat{x}(s^*)$ in (13) is due to the fact that the conditional mean $\mathbb{E}[x(s^*) | \mathbf{y}_n]$ obtains the minimum MSE for any estimator of $x(s^*)$ that is a function of \mathbf{y}_n . This estimator is not linear, and MCMC methods are necessary for evaluating (13) as the density for the conditional distribution $\pi(\mathbf{u}_n | \mathbf{y}_n)$ will not be available in closed form (no possible ‘‘conjugate’’ form for the distribution of \mathbf{u}_n is known to us). When

model parameters, such as in the covariance function c or the distribution of u are unknown, the distribution $\pi(\mathbf{u}_n|\mathbf{y}_n)$ implicitly averages over the posterior distributions of such parameters.

MCMC methods also allow us to compute prediction intervals $(z_{\text{low}}, z_{\text{high}})$ such that $\mathbb{P}(z_{\text{low}} < x(s^*) < z_{\text{high}}|\mathbf{y}_n) = 1 - \alpha$. When the covariance function c and location error model g are known, these intervals are exact probability conditional probability statements, providing a stronger coverage guarantee than that achieved with the KALE procedure in Proposition 3.3, where coverage is achieved only by averaging over \mathbf{y}_n .

4.1 Distributional Assumptions

MCMC inference for (13) requires the assumption that \mathbf{x}_n is Gaussian. While this is a common assumption in practice and has been assumed throughout this paper, it is not necessary to derive the KALE equations and their MSE (but it is necessary to produce coverage intervals as in Proposition 3.3). Thus, Kriging approaches, including KALE, are attractive when there is information about the joint distribution of x beyond its first two moments.

In this scenario, however, we can still advocate—from a decision-theoretic perspective—a Gaussian assumption when the goal of the analysis is minimum MSE prediction. Specifically, let $\pi \in \Pi_{\mathbf{0}, \mathbf{C}}$ be a choice of joint distribution for \mathbf{x}_n with the appropriate first two moments $\mathbf{0}$ and \mathbf{C} . The minimum MSE prediction of $x(s^*)$ assuming $\mathbf{x}_n \sim \pi$ is the conditional mean $\mathbb{E}_\pi[x(s^*)|\mathbf{x}_n]$. Let $R_{\pi_0}(\pi)$ be the risk (MSE) of this minimum MSE predictor under the assumption that $\mathbf{x}_n \sim \pi$ when in fact $\mathbf{x}_n \sim \pi_0$; that is,

$$R_{\pi_0}(\pi) = \mathbb{E}_{\pi_0}[(\mathbb{E}_\pi[x(s^*)|\mathbf{x}_n] - x(s^*))^2].$$

Thus $R_{\pi_0}(\pi)$ represents the risk (MSE) in a misspecified joint distribution for \mathbf{x}_n , where the analyst assumes $\mathbf{x}_n \sim \pi$, but in fact $\mathbf{x}_n \sim \pi_0$. We then have the following proposition, based on Theorem 5.5 of Morris (1983):

PROPOSITION 4.1. *Let $\pi_0 \in \Pi_{\mathbf{0}, \mathbf{C}}$ be Gaussian. Then for all $\pi \in \Pi_{\mathbf{0}, \mathbf{C}}$ we have*

$$R_\pi(\pi) \leq R_\pi(\pi_0) = R_{\pi_0}(\pi_0) \leq R_{\pi_0}(\pi).$$

Unlike traditional decision theory problems, here we are fixing the estimator (Kriging), and considering the costs of different distributional assumptions (π). Given that the analyst has decided to use Kriging for predicting $x(s^*)$, then the risk in making an incorrect distributional assumption is $R_{\pi_0}(\pi_0) - R_\pi(\pi_0) = 0$. This reflects the fact that the Kriging MSE depends only on the first two moments of π . However, there is an “opportunity cost” in making any non-Gaussian assumption $R_\pi(\pi_0) - R_\pi(\pi) > 0$ for $\pi \neq \pi_0$, which represents the reduction in MSE under π that could be achieved by using a different estimator other than Kriging.

Obviously, if there is a strong reason to believe a non-Gaussian π is true, then analysis should proceed with this assumption, ideally leveraging an estimator that is optimal under these assumptions (instead of Kriging). However, without strong distributional knowledge, the analyst can assume Gaussianity without risking increased MSE or paying an opportunity cost for using an inefficient method.

4.2 Hybrid Monte Carlo

Hybrid Monte Carlo [Neal (2005)] is well-suited for the problem of sampling $\pi(\mathbf{u}_n|\mathbf{y}_n) \propto \pi(\mathbf{y}_n|\mathbf{u}_n)\pi(\mathbf{u}_n)$ in order to evaluate (13). This is because while $\pi(\mathbf{u}_n|\mathbf{y}_n)$ is computationally expensive (requiring inversion of the covariance matrix $\mathbf{C}_\theta(\mathbf{u}_n) = \mathbf{C}_\theta(\mathbf{s}_n + \mathbf{u}_n, \mathbf{s}_n + \mathbf{u}_n)$), the gradient $\nabla \log(\pi(\mathbf{u}_n|\mathbf{y}_n))$ is a relatively cheap byproduct of this calculation. Often the conditional distribution $\mathbf{u}_n|\mathbf{y}_n$ is correlated across components, making gradient-based MCMC methods more efficient for generating samples. Other gradient-based MCMC sampling methods, such as the Metropolis-adjusted Langevin algorithm [Roberts et al. (2001)] and variants, may also be well-suited to this problem.

Bayes rule provides $\pi(\theta, \mathbf{u}_n|\mathbf{y}_n) \propto \pi(\mathbf{y}_n|\theta, \mathbf{u}_n)\pi(\theta, \mathbf{u}_n)$, where θ here represents any unknown parameter(s) of the covariance function c . In most situations it will be reasonable to assume \mathbf{u}_n and θ are independent a priori—this is trivially true in the case that θ is assumed known. Assuming this, and recognizing that $\pi(\mathbf{y}_n|\theta, \mathbf{u}_n)$ is Gaussian, we can write the log posterior and its gradient:

$$\begin{aligned} \log(\pi(\theta, \mathbf{u}_n|\mathbf{y}_n)) &= -\frac{1}{2} \log(|\mathbf{C}_\theta(\mathbf{u}_n)|) - \frac{1}{2} \mathbf{y}_n' \mathbf{C}_\theta(\mathbf{u}_n)^{-1} \mathbf{y}_n + \text{const.} \\ \frac{\partial}{\partial u_i} \log(\pi(\theta, \mathbf{u}_n|\mathbf{y}_n)) &= \\ &\frac{1}{2} \text{Tr} \left(\mathbf{C}_\theta(\mathbf{u}_n)^{-1} \left[\frac{\partial}{\partial u_i} \mathbf{C}_\theta(\mathbf{u}_n) \right] (\mathbf{C}_\theta(\mathbf{u}_n)^{-1} \mathbf{y}_n \mathbf{y}_n' - \mathbf{I}_n) \right) + \frac{\partial}{\partial u_i} \log(\pi(\mathbf{u}_n)) \\ \frac{\partial}{\partial \theta_i} \log(\pi(\theta, \mathbf{u}_n|\mathbf{y}_n)) &= \\ &\frac{1}{2} \text{Tr} \left(\mathbf{C}_\theta(\mathbf{u}_n)^{-1} \left[\frac{\partial}{\partial \theta_i} \mathbf{C}_\theta(\mathbf{u}_n) \right] (\mathbf{C}_\theta(\mathbf{u}_n)^{-1} \mathbf{y}_n \mathbf{y}_n' - \mathbf{I}_n) \right) + \frac{\partial}{\partial \theta_i} \log(\pi(\theta)). \end{aligned}$$

The computational cost of both the likelihood and gradient are dominated by solving $\mathbf{C}_\theta(\mathbf{u}_n)$ (*e.g.*, Cholesky factorization), which is $\mathcal{O}(n^3)$. Every likelihood evaluation computes this term, which can then be re-used in the gradient equations. Thus, the computational cost of computing both the likelihood and gradient remains $\mathcal{O}(n^3)$.

4.3 Multimodality

The posterior distribution $\pi(\theta, \mathbf{u}_n|\mathbf{y}_n)$ is often multimodal, more so if the distribution $\pi(\mathbf{u}_n)$ is diffuse. This is because if there is a local mode at $(\hat{\theta}, \hat{\mathbf{u}}_n)$, there may be a local mode at any (θ, \mathbf{u}_n) such that $\mathbf{C}_\theta(\mathbf{u}_n) = \mathbf{C}_{\hat{\theta}}(\hat{\mathbf{u}}_n)$, as the likelihood is constant for such (θ, \mathbf{u}_n) . In particular, for isotropic covariance models, the likelihood is constant for additive shifts in \mathbf{u}_n or rotations of $\mathbf{s}_n + \mathbf{u}_n$, as these operations preserve pairwise distances. Additionally, multimodality can be induced by the many-to-one mapping of the set of true locations $\{s_i + u_i, i = 1, \dots, n\}$ to the set of observed locations $\{s_i, i = 1, \dots, n\}$. For instance, with $n = 2$ and an isotropic covariance function, for any choice of u_1, u_2 we get the same likelihood with $\tilde{u}_1 = s_2 + u_2 - s_1$ and $\tilde{u}_2 = s_1 + u_1 - s_2$. Moreover, for fixed \mathbf{u}_n , for many common covariance functions it is possible for the posterior of θ to be multimodal [Warnes and Ripley (1987)].

HMC (and other gradient MCMC methods) can efficiently sample from multiple modes, however this becomes difficult when the modes are isolated by regions of extremely low likelihood [Neal (2011)]. Isolated modes can occur in the

location-error GP regime. For example, assume one-dimensional locations ($p = 1$) and an isotropic covariance model with known parameters θ and nugget σ_x^2 . Marginally, as $\|s_1 + u_1 - (s_2 + u_2)\| \rightarrow 0$, $y_1 - y_2 \xrightarrow{D} \mathcal{N}(0, 2\sigma_x^2)$; that is, the scaled difference $|y_1 - y_2|/(\sigma_x)$ must be reasonably small. When this is not the case (e.g. $\sigma_x^2 = 0$), then the log-likelihood asymptotes at $s_1 + u_1 = s_2 + u_2$ almost surely. Thus, the Markov chain can only sample \mathbf{u}_n such that the ordering of $\{s_i + u_i, i = 1, \dots, n\}$ is preserved. Note that when $p > 1$, while the log-likelihood may still asymptote at $s_1 + u_1 = s_2 + u_2$, this no longer constrains the space of \mathbf{u}_n (except on sets with measure 0).

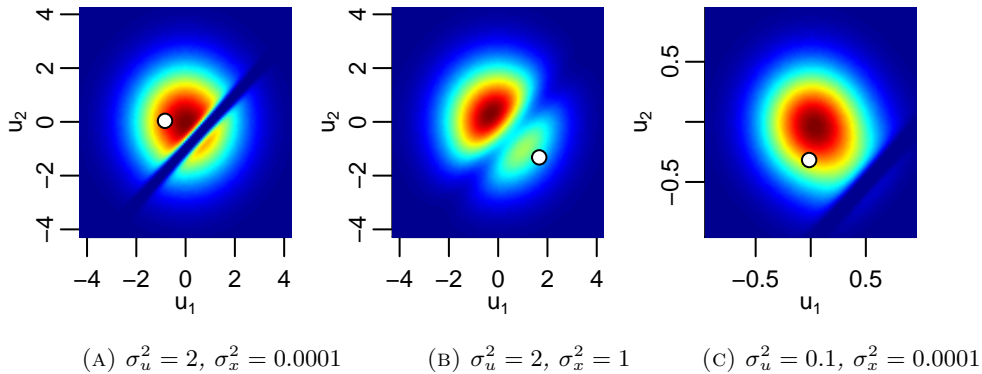


FIG 4. Density of (u_1, u_2) using the covariance function $c(s_1, s_2) = \exp(-(s_1 - s_2)^2) + \sigma_x^2 \mathbf{1}_{s_1=s_2}$. We simulate data (y_1, y_2) using $s_1 = 0, s_2 = 1$, and $u_i \sim \mathcal{N}(0, \sigma_u^2)$, and different values of σ_x^2 and σ_u^2 .

Figure 4 demonstrates the modal behavior for this simple example with $p = 1$ and $n = 2$. When location errors are large in magnitude and the nugget term σ_x^2 is small, the modes of (u_1, u_2) are separated by a contour of near 0 density (panel A). A higher nugget σ_x^2 increases the density between the modes, making it easier for the same MCMC chain to travel between them (panel B). Decreasing the magnitude of the (Gaussian) location errors, σ_u^2 , puts more mass on a single mode, as the unimodal distribution $\pi(\mathbf{u}_n)$ has a greater influence on $\pi(\mathbf{u}_n|\mathbf{y}_n)$ (panel C).

Thus, as with any MCMC application, for the location-error GP problem it is advisable to run separate chains in parallel, with different, diffuse starting points, and monitor mixing diagnostics [Gelman and Shirley (2011)]. Multiple chains failing to mix is likely a symptom of multiple isolated modes, in which case we should modify the HMC algorithm to include tempering [Salazar and Toral (1997)] or non-local proposals that allow for mode switching [Qin and Liu (2001), Lan, Streets and Shahbaba (2013)]. Another strategy to overcome multiple isolated modes is importance sampling: as Figure 4 shows, increasing the nugget variance σ_x^2 increases the density between modes. If we generate samples according to $\tilde{\pi}(\theta, \mathbf{u}_n|\mathbf{y}_n) \propto \tilde{\pi}(\mathbf{y}_n|\theta, \mathbf{u}_n)\pi(\theta)\pi(\mathbf{u}_n)$ where $\tilde{\pi}(\mathbf{y}_n|\theta, \mathbf{u}_n)$ is the density corresponding to $\mathcal{N}(\mathbf{0}, \mathbf{C}_\theta(\mathbf{u}_n) + \kappa\mathbf{I}_n)$ for some fixed κ , then it is straightforward to compute importance weights $\pi(\theta, \mathbf{u}_n|\mathbf{y}_n)/\tilde{\pi}(\theta, \mathbf{u}_n|\mathbf{y}_n)$. This is because $\mathbf{C}_\theta(\mathbf{u}_n)^{-1}$ is easy to compute from $(\mathbf{C}_\theta(\mathbf{u}_n) + \kappa\mathbf{I}_n)^{-1}$ (and vice versa) using the Woodbury formula. Either standard importance sampling, or Hamiltonian importance sampling [Neal (2005)], could be used to generate parameter estimates, point/interval predictions, and any other posterior estimates of interest.

Parameter	Values simulated	Prior support
τ^2	1	(0, 10)
β	0.001, 0.01, 0.1, 0.5, 1, 2	(0.0005, 3)
σ_x^2	0.0001, 0.01, 0.1, 0.5, 1	(0, 10)
σ_u^2	0.0001, 0.01, 0.1, 0.5, 1	(0, 10)

TABLE 1

Parameter values used in simulation study. The range (0.0005, 3) for β guarantees that at least one pair of points among our observed data has a correlation in the range (0.05, 0.95). This eliminates modes corresponding to white noise processes from the likelihood surface.

5. SIMULATION STUDY

We compare Kriging (both KALE and KILE) and HMC methods for point/interval forecasts for Gaussian process regression in a simulation study. For various combinations of parameter values for the covariance function $c(s_1, s_2)$ and location error model $g(u)$ we simulate observations \mathbf{y}_n where $y_i = x(s_i + u_i)$ and make predictions for values of x at unobserved locations: $\mathbf{x}_k^* = (x(s_1^*) \dots x(s_k^*))'$.

We simulate data using the squared exponential covariance function $c(s_1, s_2) = \tau^2 \exp(-\beta \|s_1 - s_2\|^2) + \sigma_x^2 \mathbf{1}_{s_1=s_2}$ and an i.i.d. Gaussian location error model $u_i \stackrel{iid}{\sim} \mathcal{N}(0, \sigma_u^2 \mathbf{I}_p)$. The squared exponential covariance function and Gaussian location error model combine to form a convenient regime, as we can evaluate k in closed form (5). Without loss of generality, we can use $\tau^2 = 1$ for all simulations as it is simply a scale parameter. We consider a $p = 2$ dimensional location space, $s_i \in \mathbb{R}^2$. On a 8×8 grid, we randomly select 54 locations at which we observe y , and target the remaining 10 locations for interpolating x . Figure 5 illustrates a range of data samples for processes used in our simulations on this space, while Table 1 provides a full summary of all the parameter value combinations we consider. Data from each parameter combination is simulated 100 times.

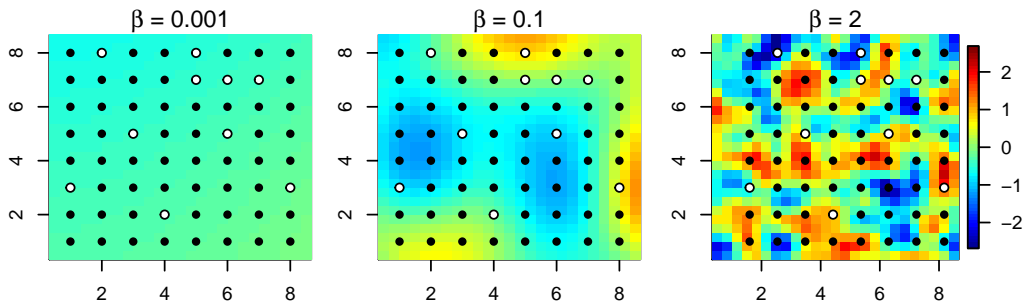


FIG 5. Samples of $x(s)$ for different values of the length-scale parameter β with the squared exponential covariance function, $c(s_1, s_2) = \exp(-\beta \|s_1 - s_2\|^2) + \sigma_x^2 \mathbf{1}_{s_1=s_2}$. Black points are where we have observed $y(s)$ and white points are where we wish to predict $x(s)$. Observed/predicted locations were randomly sampled from an 8×8 grid.

We evaluate the three prediction methods—KALE, KILE, and HMC—using both adjusted root mean squared error (RMSE) and the coverage probability of a 95% interval. “Adjusted” RMSE is based on the MSE with σ_x^2 subtracted out, as this term appears in the MSE for any prediction method. For every parameter combination of interest used, these statistics are calculated first by averaging over each of the $k = 10$ prediction targets in each simulated draw of new data, and then over the $J = 100$ independent data draws.

Both evaluation statistics can be evaluated more precisely during simulation by utilizing a simple Rao-Blackwellization. For iteration j , instead of drawing \mathbf{x}_k^* in addition to \mathbf{y}_n and calculating $\text{rmse}_j = \|\mathbf{x}_k^* - \hat{\mathbf{x}}_k^*\|/k$, we simply condition on the simulated location errors \mathbf{u}_n to get $\text{rmse}_j = \mathbb{E}[\|\mathbf{x}_k^* - \hat{\mathbf{x}}_k^*\|/k \mid \mathbf{y}_n, \mathbf{u}_n]$. Similarly, to calculate coverage of an interval $(L_{s^*}(\mathbf{y}_n), U_{s^*}(\mathbf{y}_n))$ for $x(s^*)$, for iteration j we use

$$\text{cov}_j = \frac{1}{k} \sum_{i=1}^k \mathbb{E}[\mathbf{1}[x(s_i^*) \in (L_{s_i^*}(\mathbf{y}_n), U_{s_i^*}(\mathbf{y}_n))] \mid \mathbf{y}_n, \mathbf{u}_n].$$

HMC is implemented using the software `RStan` [Stan Development Team (2014)], which implements the “no-U-turn” HMC sampler [Homan and Gelman (2014)]. 10000 samples were drawn during each simulation iteration, which (for most parameter values) takes a few minutes on a single 2.50Ghz processor.

5.1 Known covariance parameters

We first simulate point and interval prediction for KALE, KILE, and HMC using the same parameter values that generated the data. By doing so, we leave aside the issue of parameter inference and simply compare the extent to which different methods leverage the information in the location-error corrupted data \mathbf{y}_n to infer $x(s^*)$. Figure 6 compares RMSE for the three methods when there is a very small nugget, $\sigma_x^2 = 0.0001$.

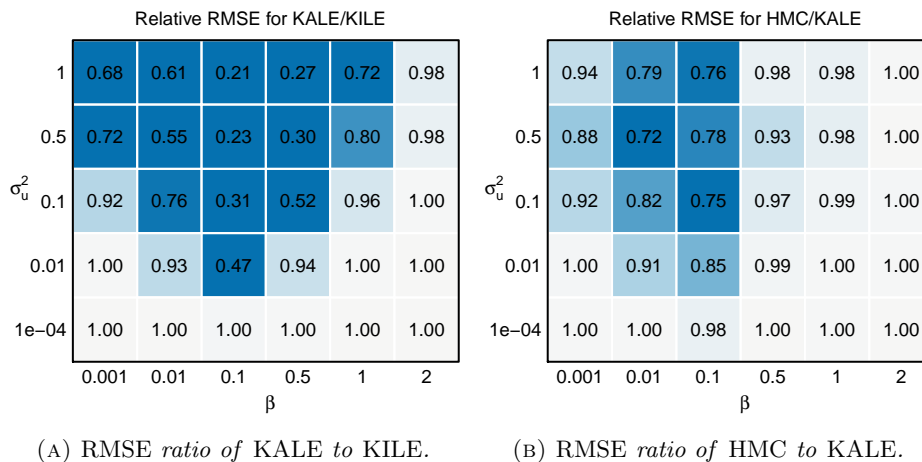


FIG 6. Relative RMSE of KALE and KILE (A) and HMC and KALE (B) for each combination of parameters (β, σ_u^2) indicated, and $\sigma_x^2 = 0.0001$. Blue shading represents a relative decrease in RMSE while red shading represents a relative increase in RMSE.

We can see that there is little difference among the three methods when σ_u^2 is sufficiently small (0.0001), or when β is sufficiently large (2). This makes sense, as in the former case, with small location errors the potential improvement over KILE (which is exact for $\sigma_u^2 = 0$) is negligible, and in the latter case, observations are too weakly correlated for nearby points to be informative. Larger values of σ_u^2 give KALE a significant reduction in RMSE versus KILE, with the reduction as large as 79% for the case of large magnitude location errors ($\sigma_u^2 = 1$) and a moderately smooth signal ($\beta = 0.1$).

The idea of a moderately smooth signal requires further elaboration: for a

given σ_u^2 , when x is very smooth (β very small), the process is roughly constant within small neighborhoods, meaning $y(s) \approx x(s)$ and location errors are less of a concern for accurate inference and prediction. On the other hand, when β is very large and the process is highly variable in small regions of the input space, location errors are less of a concern because there is very little information in the data to begin with. Location errors are most influential when the process x has more moderate variation across neighborhoods corresponding to the plausible range of the location errors.

HMC offers further reductions in RMSE over KALE in roughly the same regions of the parameter space in which KALE improves over KILE, although the additional improvement is less dramatic. The maximum RMSE reduction we observe is about 28%, once again for a moderately smooth signal with larger magnitude location errors.

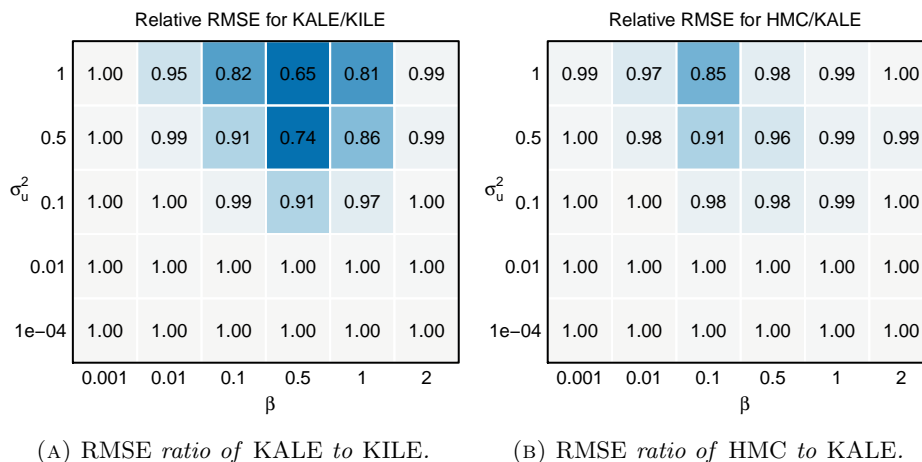


FIG 7. Relative RMSE of KALE to KILE (A) and HMC and KALE (B) for each combination of parameters (β , σ_u^2) indicated, and $\sigma_x^2 = 0.1$. Blue shading represents a relative decrease in RMSE while red shading represents a relative increase in RMSE.

When the nugget variance σ_x^2 is increased (Figure 7 shows results for $\sigma_x^2 = 0.1$), differences in RMSE among the three methods become smaller (the differences are wiped out entirely at $\sigma_x^2 = 1$, which is not pictured). This is not due to a shared σ_x^2 term in the RMSE value for all methods, as this is subtracted out. Rather, the similarity of all three methods reflects the fact that a larger nugget leaves less information in the data that can be effectively used for prediction. However, the differences that we do observe (both comparing KALE to KILE and HMC to KALE) occur primarily when the magnitude of location errors σ_u^2 is large.

In the case where all parameters are fixed and known, both KALE and HMC produce intervals with exact coverage (subject to Monte Carlo or numerical approximation errors) in all simulations. KILE, however, can severely undercover in the presence of location errors. Figure 8 shows coverage as low as 4% when the magnitude of the location errors is high ($\sigma_u^2 = 1$), $\beta = 0.1$, and the nugget variation is minimal ($\sigma_x^2 = 0.0001$). Undercoverage still persists in this region of the parameter space for $\sigma_x^2 = 1$, the largest nugget variance used in our simulations.

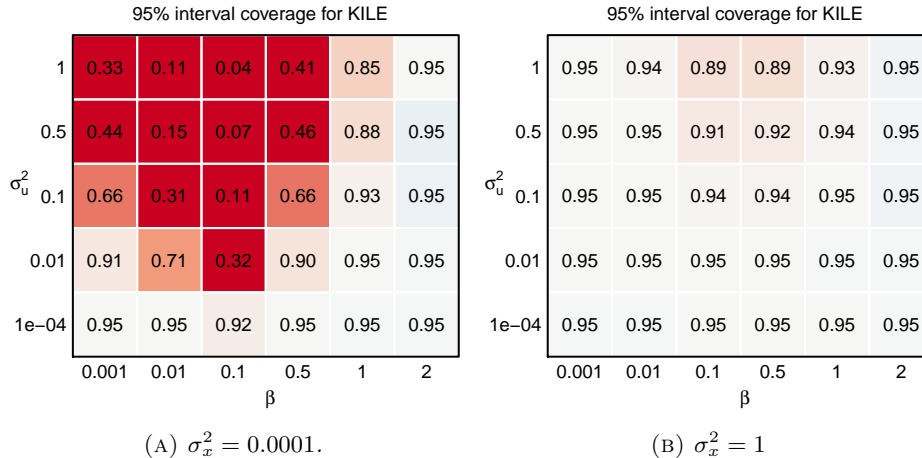


FIG 8. 95% interval coverage for KILE for $\sigma_x^2 = 0.0001$ (A) and $\sigma_x^2 = 1$ (B). With moderately smooth signals and large location errors, we see severe undercoverage that does not disappear even for $\sigma_x^2 = 1$.

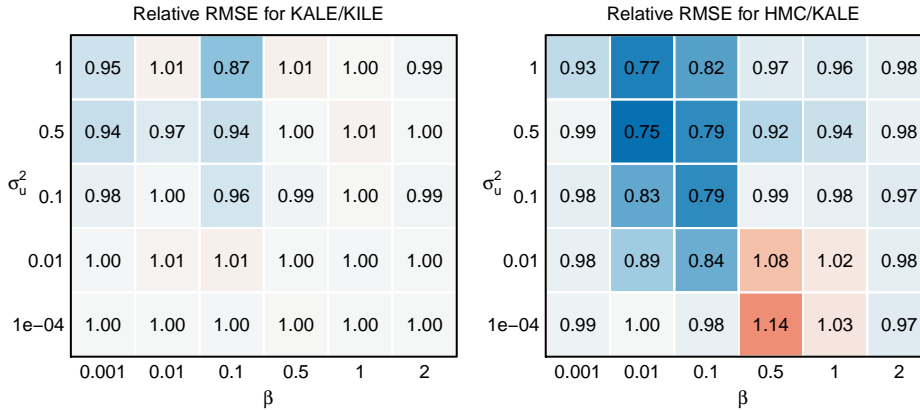
5.2 Unknown covariance parameters

In typical applied settings, the analyst will not know model parameters such as those of the covariance function (τ^2, β) , the nugget variance σ_x^2 , or even the variance of the location errors σ_u^2 . Due to identifiability issues with our choice of covariance function in this simulation (5), we assume σ_u^2 is known but estimate all other parameters before making predictions at unobserved locations.

For KILE and KALE, parameter estimation is accomplished through maximum (pseudo-) likelihood, as in (8). Parameter estimates are then plugged into Kriging equations (4)–(7) to obtain corresponding point and interval estimates. Because c and k are both squared exponential (5), the pseudolikelihood estimation procedure estimates the same covariance function for y , however the estimated parameters (and therefore Kriging equations, based on k^*) will differ. The plug-in approach ignores uncertainty in parameter estimates, so plug-in MSE estimates will be too optimistic. Various techniques exist for adjusting MSE from estimated parameters [Smith (2004), Zhu and Stein (2006)], though there is no need to incorporate such techniques into our analysis since exact (up to Monte Carlo error) MSEs are provided by simulation.

For HMC, we supply unknown parameters with prior distributions and sample parameters and predictions jointly from the posterior distribution $\pi(\theta, \mathbf{x}_k^* | \mathbf{y}_n)$. The priors we use are flat over a reasonable range (see Table 1), which guarantees both a proper posterior and a posterior mode that agrees with the maximum likelihood estimate of θ . This second condition supports fair comparisons between predictions derived from HMC parameter estimates versus those based on the maximum (psueolikelihood) parameter values.

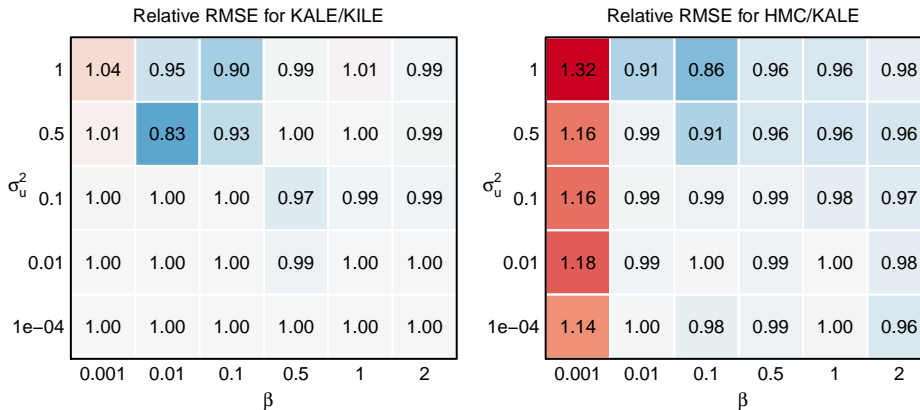
Figure 9 provides the relative RMSE of KALE *vs.* KILE, and HMC *vs.* KALE, for predictions when parameters must first be estimated (using $\sigma_x^2 = 0.0001$). We notice that there does not appear to be a great advantage in KALE over KILE when parameters are first estimated. This is because, as mentioned earlier, the marginal process y still has a squared exponential covariance function 5, so Kriging equations for KALE and KILE will be very similar. On the other hand,



(A) RMSE ratio of KALE to KILE. (B) RMSE ratio of HMC to KALE.

FIG 9. Relative RMSE of KALE and KILE (A) and HMC and KALE (B) for each combination of parameters (β, σ_u^2) indicated, and $\sigma_x^2 = 0.0001$. Parameters are assumed unknown and first estimated to obtain point predictions.

we notice a modest improvement when using HMC over Kriging, except in a small region of the parameter space ($\sigma_u^2 \leq .01$ and $\beta \in [0.5, 1]$).



(A) RMSE ratio of KALE to KILE. (B) RMSE ratio of HMC to KALE.

FIG 10. Relative RMSE of KALE and KILE (A) and HMC and KALE (B) for each combination of parameters (β, σ_u^2) indicated, and $\sigma_x^2 = 0.1$. Parameters are assumed unknown and first estimated to obtain point predictions.

When the nugget variance is increased to $\sigma_x^2 = 0.1$, we see the results in Figure 10. We still see relatively similar performances from KALE and KILE. HMC offers a small improvement over KALE when $\beta \geq 0.01$, though for $\beta = 0.001$ we actually see significantly higher MSEs with HMC. At $\beta = 0.001$ the process is extremely smooth, as the most distant pairs of observations still have a correlation of 0.88. We are thus more concerned with overestimating β than underestimating it; as the former shrinks predictions towards 0 while the latter shrinks towards (approximately) the mean of all observations. As we use a flat prior for β , where almost all mass is located $\beta > .001$, the posterior tends to overestimate β , leading

to draws with relatively high MSE.

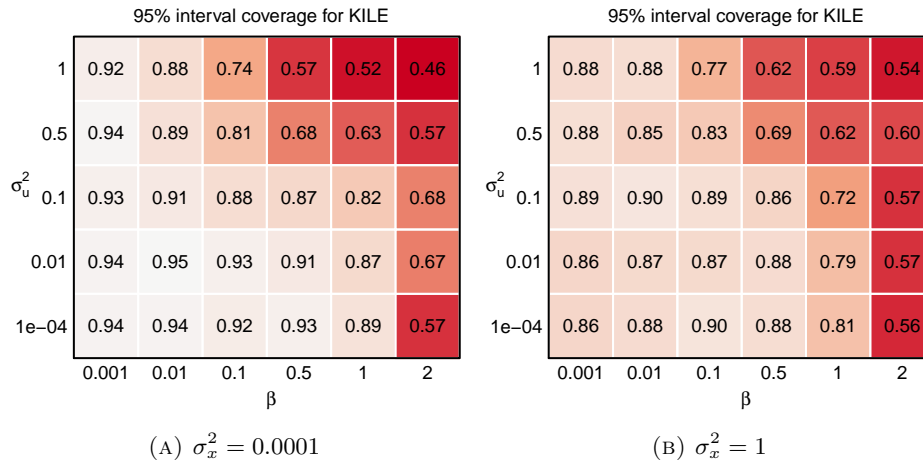


FIG 11. 95% interval coverage for KILE for $\sigma_x^2 = 0.0001$ (A) and $\sigma_x^2 = 1$ (B).

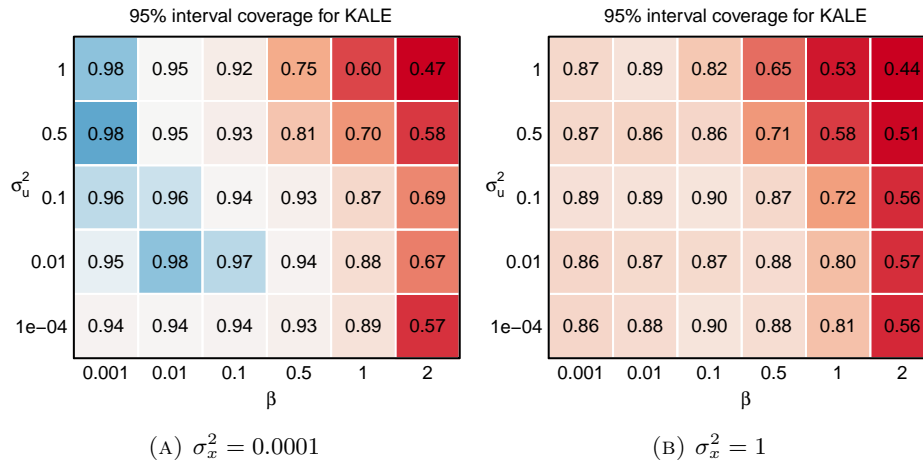


FIG 12. 95% interval coverage for KALE for $\sigma_x^2 = 0.0001$ (A) and $\sigma_x^2 = 1$ (B).

Neither Kriging or HMC guarantees prediction intervals with the correct coverage in the regime where parameters must first be estimated (though HMC would give proper “Bayes coverage” when simulating θ according to the prior used). We nevertheless present coverage results in Figures 11–13. While we do not expect any method used to provide exact coverage, Kriging (both KALE and KILE) suffer from significant undercoverage for some regions of the parameter space, while HMC is consistent in offering at least 85% coverage throughout our simulations. In a regime without location errors, Zimmerman and Cressie (1992) advocate Bayesian procedures under non-informative priors over frequentist procedures in order to obtain interval estimates with good coverage; our simulation results, albeit in the context of location errors, agree with this finding.

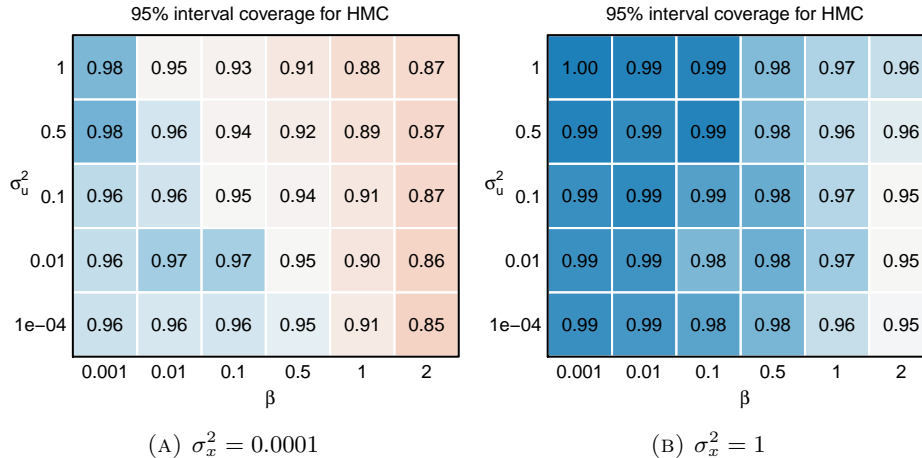


FIG 13. 95% interval coverage for HMC for $\sigma_x^2 = 0.0001$ (A) and $\sigma_x^2 = 1$ (B).

5.3 Summary

Our simulation results confirm the theoretical guarantee of KALE dominating KILE in prediction MSE when the covariance function is known, and furthermore HMC dominating KALE. The magnitude of differences in MSE between these methods is greatest when the process is moderately smooth relative to the spatial sampling (*e.g.*, $0.01 \leq \beta \leq 0.5$), when the magnitude of location errors σ_u^2 is largest, and when nugget variation σ_x^2 is smallest. For such regions of the parameter space, KILE fails to deliver prediction intervals with proper coverage, whereas KALE and HMC can give valid prediction intervals for any parameter values.

An important consequence in adjusting for location errors with a known covariance function is the corresponding adjustment to the nugget. The discussion in (Sections 3.6 and 3.7 of) Stein (1999) emphasizes the importance of correctly specifying the high-frequency behavior of the process when interpolating (correctly specifying the low-frequency behavior is less crucial), including the nugget term. Estimating parameters, including the nugget term σ_x^2 , implicitly corrects for model misspecification when ignoring location errors. Thus we see little difference in predictive performance between KALE and KILE when parameters are first estimated. Depending on the choice of prior, KALE/KILE may give lower MSE predictions than HMC, which averages over posterior parameter uncertainty; however, interval coverage is better for HMC (using weak prior information) than for KALE/KILE.

6. INTERPOLATING NORTHERN HEMISPHERE TEMPERATURE ANOMOLIES

To illustrate the methods discussed in this paper, we consider interpolating northern hemisphere temperature anomalies during the summer of 2011 using the publicly available CRUTEM3v data set¹ [Brohan et al. (2006)]. Figure 14 shows our data. These data are used in geostatistical reconstructions of the Earth's

¹<http://www.cru.uea.ac.uk/cru/data/temperature/>

temperature field, which interpolate temperatures at unobserved points in space-time in order to better understand the historical behavior of climate change (see, *e.g.*, [Tingley and Huybers \(2010\)](#) and [Richard et al. \(2012\)](#)). Each observation is a spatiotemporal average: temperature readings are averaged over the April–September period and each $5^\circ \times 5^\circ$ longitude-latitude grid cell. These values are then expressed as anomalies relative to the global average during the period 1850–2009, which is calculated using an ANOVA model [[Tingley \(2012\)](#)]. Apart from this spatiotemporal averaging, numerous other preprocessing steps adjust this data for differences in altitude, timing, equipment, and measurement practices between sites, along with other potential sources of error; please see [Morice et al. \(2012\)](#) and [Jones et al. \(2012\)](#) for more details.

Our analysis, restricted to interpolating a single year of data, and without using external data such as temperature proxies [[Mann et al. \(2008\)](#)], is intended as a proof of concept rather than as a refinement or improvement to existing analyses of these data. We wish to illustrate the potential impact of location errors on conclusions drawn from these data.

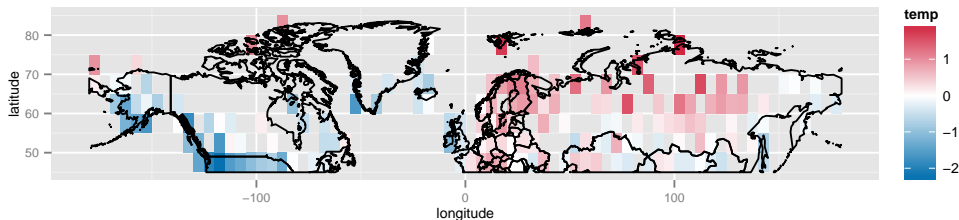


FIG 14. *CRUTEM3v* data for summer 2011, with 2011 mean subtracted so that measurements represent spatial anomalies. Generally speaking, we see lower (cooler) anomalies in North America and positive (warmer) anomalies in Europe. Higher latitudes also tend to have positive anomalies.

The “gridding”, or spatial averaging across $5^\circ \times 5^\circ$ cells, complicates analyses using Gaussian process models [[Director and Bornn \(2015\)](#)]. However, assuming a smooth temperature field, we know that the recorded spatial average must be realized exactly at some location in each grid box (closer to the center if a lot of points have been averaged together). This frames the spatial averaging problem as a location measurement error problem: instead of observing the temperature $x(s)$ at each grid center s , we observe the temperature at an unknown location displaced from the grid center: $y(s) = x(s + u)$.

Following [Tingley and Huybers \(2010\)](#), we assume an exponential covariance function for $x(s)$, where distance is calculated along the Earth’s surface. As s is given in terms of longitude/latitude ($s = (\psi, \phi)$), this has the form

$$c(s_1, s_2) = \tau^2 \exp(-\beta \Delta) + \sigma_x^2 \mathbf{1}_{s_1=s_2}$$

$$(14) \quad \Delta = 2r \arcsin \sqrt{\sin^2 \left(\frac{\phi_2 - \phi_1}{2} \right) + \cos(\phi_1) \cos(\phi_2) \sin^2 \left(\frac{\psi_2 - \psi_1}{2} \right)},$$

where $r = 6371$ is the radius of the earth (in km). At higher latitudes (ϕ), the centers of each grid cell are closer together, so nearby observations are more strongly correlated. The nugget term σ_x^2 represents some combination of measurement error in temperature readings and high-frequency spatial variation that

is inestimable using the gridded observation samples.

We assume the following model for location errors u_i , which are additive displacements of longitude/latitude coordinates $s_i = (\psi_i, \phi_i)$:

$$(15) \quad u_i \sim \mathcal{N} \left(\mathbf{0}, \sigma_u^2 \left(\frac{180}{\pi r} \right)^2 \begin{pmatrix} \frac{1}{\cos^2(\phi_i)} & 0 \\ 0 & 1 \end{pmatrix} \right).$$

This prior is equivalent to assuming that distance along the Earth’s surface (great-circle distance) between each grid center and the corresponding observation location has a scaled chi distribution, $d(s_i, s_i + u_i) \sim \sigma_u \chi$. Combining (15) and (14), we use Monte Carlo to compute k .

We treat parameters $\tau^2, \beta, \sigma_x^2$ as unknown, but fix $\sigma_u^2 = 7500$. At this value, the median magnitude of the location errors in great-circle distance is 102km, which is consistent with analyzing the coordinates of the temperature recording sites used to compile the CRUTEM3v data².

6.1 Kriging

We first apply Kriging approaches to interpolate the CRUTEM3v data, both adjusting for and ignoring location errors (15). Because parameters $\tau^2, \beta, \sigma_x^2$ are unknown, we first need to estimate them using maximum likelihood (when ignoring location errors) or maximum pseudo-likelihood (8) (when adjusting for location errors). These can then be plugged in to covariance functions c and k to obtain “empirical” Kriging equations we can use for interpolation [Zimmerman and Cressie (1992)].

We find small differences in parameter estimates when ignoring location errors (assuming $\sigma_u^2 = 0$) and adjusting for them (assuming $\sigma_u^2 = 7500$):

σ_u^2	$\hat{\tau}^2$	$\hat{\beta}$	$\hat{\sigma}_x^2$
0	1.1671	1.4275×10^{-4}	0.0747
7500	1.1649	1.4677×10^{-4}	0.0699

TABLE 2

Covariance function parameter estimates when ignoring location errors (assuming $\sigma_u^2 = 0$) and adjusting for location errors (assuming $\sigma_u^2 = 7500$).

Consequently, when we interpolate data at the centers of grid cells for which no data was observed, we see differences between the KALE and KILE approaches. Figure 15 shows the differences between KALE and KILE interpolations (both point and interval estimates). Relative to the range of the data (most anomalies are in the interval $(-1, 1)$), the discrepancy between KALE and KILE does not seem very significant.

6.2 HMC

Using HMC, parameter inference and interpolations are made simultaneously. The resulting point and interval predictions differ substantially from the Kriging results. However, because HMC incorporates parameter uncertainty in predictions, this comparison is not sufficient to illustrate the impact of location errors on conclusions from this data. A more appropriate comparison is between HMC

²Station locations are viewable at <https://www.ncdc.noaa.gov/oa/climate/ghcn-daily/>

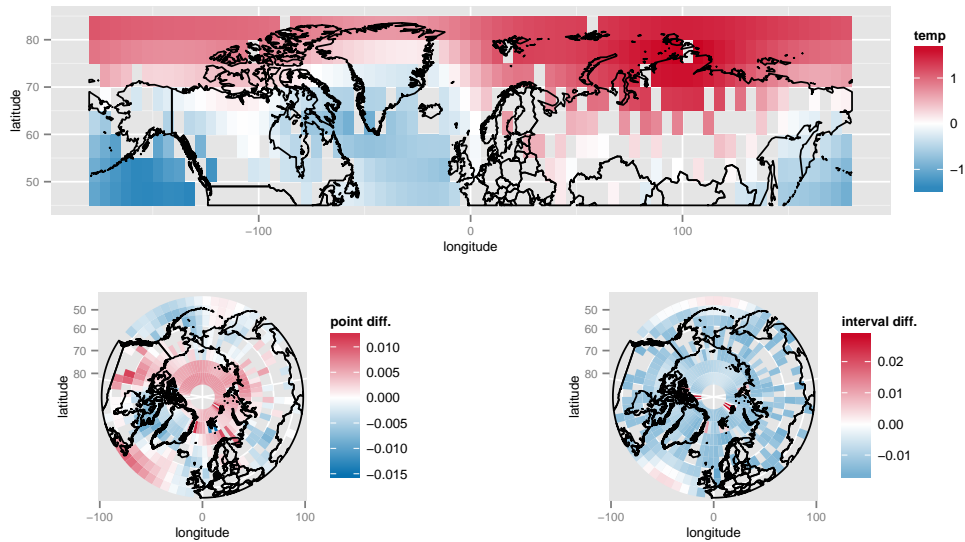


FIG 15. Kriging results for interpolating temperature anomalies from summer 2011. The top plot shows interpolations at unobserved grid centers given by KALE. The bottom left plot shows the difference in estimates between KALE and KILE (KALE - KILE), and the bottom right plot shows difference in 95% interval widths between KALE and KILE.

with a location error model ($\sigma_u^2 = 7500$), and HMC assuming with no location errors ($\sigma_u^2 = 0$). These results are plotted in Figure 16.

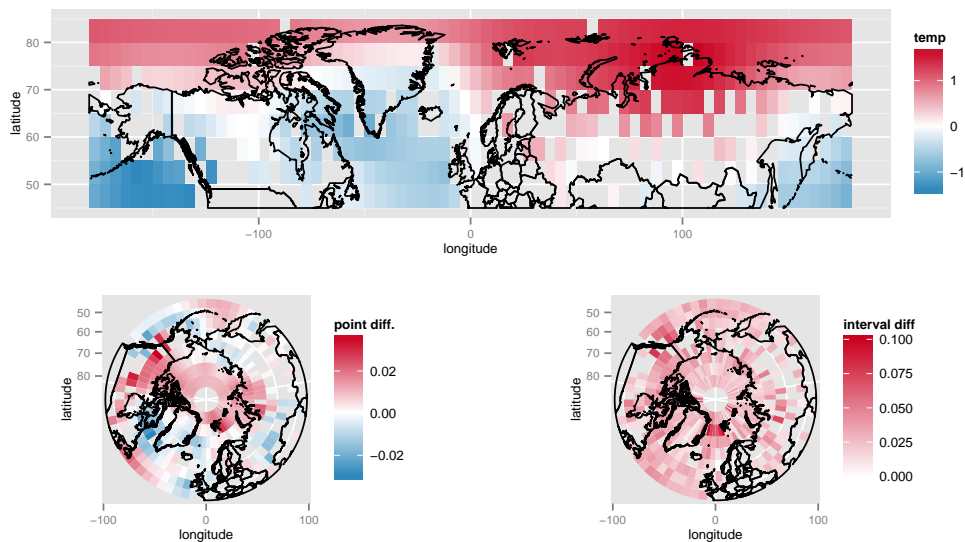


FIG 16. Results for interpolating temperature anomalies from summer 2011 using HMC. The top plot shows interpolations at unobserved grid centers, assuming location errors $\sigma_u^2 = 7500$. The bottom left plot shows the difference in estimates between the location error model and the model with $\sigma_u^2 = 0$. The bottom right plot shows difference in 95% interval widths.

Using HMC, accounting for location errors produces more significant differences in inference/prediction than was observed for Kriging. This is particularly true for interval predictions, where adjusting for location errors yields intervals as much as 0.1 wider, which is a significant discrepancy when most observations lie in $(-1, 1)$.

Figure 17 shows posterior densities for unknown parameters of the covariance function based on HMC draws from the $\sigma_u^2 = 7500$ and $\sigma_u^2 = 0$ models (the Kriging estimates of these parameters are vertical lines). HMC under location error model ($\sigma_u^2 = 7500$) gives slightly larger β estimates than when using $\sigma_u^2 = 0$, meaning observations are inferred to be less strongly correlated. This yields prediction intervals that tend to be wider (see Figure 16). The most extreme discrepancies occur in the arctic, where distances between grid points are closest. The fact that modeling location errors adds additional uncertainty to arctic predictions is of particular interest to climate scientists, as accurate climate reconstruction for the arctic region is essential for understanding recent climate change patterns [Cowntan and Way (2014)].

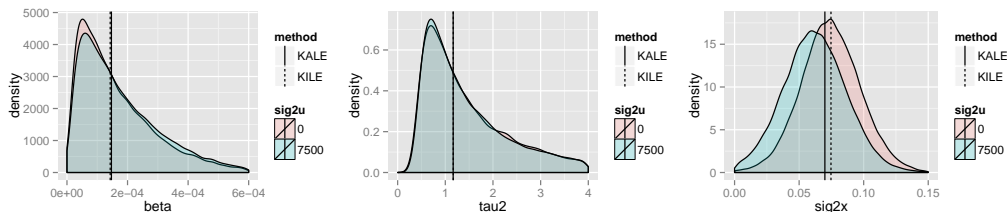


FIG 17. Density of posterior draws from HMC using $\sigma_u^2 = 7500$ (blue) and $\sigma_u^2 = 0$ (red). Point estimates of these parameters from Kriging (Table 2) are shown as vertical lines.

The difference between predictions obtained under the $\sigma_u^2 = 0$ and $\sigma_u^2 = 7500$ models using HMC suggests that modeling location errors, even when they are small in magnitude, meaningfully impacts parameter estimates and predictions at unobserved locations. The fact that results for HMC (assuming $\sigma_u^2 = 7500$) also differ from the results using KALE, while the KILE results do so less, demonstrates that moment procedures such as Kriging may be ineffective in adjusting for these errors.

7. CONCLUSION

In this paper, we have explored the issue of Gaussian process regression when locations in the input space \mathbb{S} are subject to error. Even when location errors are quite small in magnitude, it is essential to adjust Kriging equations in order to obtain good point and interval estimates; further improvements can be made by using MCMC to sample directly from the distribution of the measurement of interest given the sampled data.

Both MCMC and Kriging will be infeasible for large data sets, due to the cost of the covariance matrix inversion. A useful future study would be to adapt the procedures discussed in this paper to methods for inference and prediction for large spatial data sets, such as the predictive process approach [Banerjee et al. (2008)], low rank representations [Cressie and Johannesson (2008)], likelihood approximations [Stein, Chi and Welty (2004)], and Markov random field approximations [Lindgren, Rue and Lindström (2011)]. It will also be useful to extend the analysis of this paper to regimes where location errors may be correlated with the process of interest x . For example, in climate data, regions with extreme climates will be harder to sample, thus there may be greater error in the spatial referencing of such sampling than for regions that are easier to sample.

APPENDIX A: PROOFS OF RESULTS

A.1 Proof of Proposition 3.1

k is a valid covariance function if and only if for all n , \mathbf{s}_n , and $\{a_i \in \mathbb{R}, i = 1, \dots, n\}$, we have

$$\sum_{i=1}^n \sum_{j=1}^n a_i a_j k(s_i, s_j) \geq 0.$$

From (3), this condition can be rewritten:

$$\begin{aligned} \sum_{i=1}^n \sum_{j=1}^n a_i a_j k(s_i, s_j) &= \sum_{i=1}^n \sum_{j=1}^n a_i a_j \int_{\mathbb{S}} c(s_i + u_i, s_j + u_j) dg_{\mathbf{s}_n}(\mathbf{u}_n) \\ &= \int_{\mathbb{S}} \sum_{i=1}^n \sum_{j=1}^n a_i a_j c(s_i + u_i, s_j + u_j) dg_{\mathbf{s}_n}(\mathbf{u}_n) \end{aligned}$$

As c is a valid covariance function, the integrand in this expression is always non-negative, so the integral is also non-negative. Thus k is a valid covariance function.

Note that for the common scenario where location errors are independent, so that $g_{\mathbf{s}_n}$ is a product measure $g_{s_1} \times \dots \times g_{s_n}$, then Proposition 3.1 is a special case of kernel convolution [Rasmussen (2006)].

A.2 Proof of Proposition 3.2

Without loss of generality, we can assume $\tau^2 = 1$ and fix $\beta, \Delta > 0$. Using the fact that $k^*(s, s^*) = \mathbb{E}[\exp(-\beta \|s + u - s^*\|^2)]$, evaluating the moment generating function of a non-central χ_p^2 random variable $\|s + u - s^*\|^2$ yields

$$c(\sigma_u^2) \equiv \mathbb{E}[(\hat{x}_{\text{KALE}}(s^*) - x(s^*))^2] = 1 - \left(\frac{1}{1 + 2\beta\sigma_u^2} \right)^p \exp\left(\frac{-2\beta\Delta^2}{1 + 2\beta\sigma_u^2} \right).$$

Differentiating, we get

$$c'(\sigma_u^2) = \frac{2\beta[2\beta(p\sigma_u^2 - \Delta^2) + p]}{(1 + 2\beta\sigma_u^2)^{p+2}} \exp\left(\frac{-2\beta\Delta^2}{1 + 2\beta\sigma_u^2} \right).$$

If $\beta\Delta^2 \leq p/2$, then $c'(\sigma_u^2) > 0$ for all $\sigma_u^2 > 0$. Since $c(\sigma_u^2)$ is left continuous at 0, continuous on \mathbb{R}_+ , and $c(0) = c_0$, this means $\beta\Delta^2 \leq p/2$ implies $c(\sigma_u^2) \geq c_0$ for all σ_u^2 .

Otherwise, if $\beta\Delta^2 > p/2$, then for all $0 < \sigma_u^2 < \frac{\Delta^2}{k} - \frac{1}{2\beta}$, we have $c'(\sigma_u^2) < 0$. Once again, because $c(\sigma_u^2)$ is left continuous at 0, continuous on \mathbb{R}_+ , and $c(0) = c_0$, this means $c(\sigma_u^2) < c_0$ for σ_u^2 in this interval.

A.3 Proof of Proposition 3.3

Let $W = x(s^*) - \hat{x}_{\text{KALE}}(s^*)$. We can explicitly write the dependence of W on \mathbf{u}_n :

$$W|\mathbf{u}_n \sim \mathcal{N}(0, V(\mathbf{u}_n))$$

where

$$\begin{aligned} V(\mathbf{u}_n) &= \sigma^2 + \gamma' \mathbf{C}(\mathbf{s}_n + \mathbf{u}_n, \mathbf{s}_n + \mathbf{u}_n) \gamma - 2\gamma' \mathbf{C}(\mathbf{s}_n + \mathbf{u}_n, s^*), \\ \gamma &= \mathbf{K}(\mathbf{s}_n, \mathbf{s}_n)^{-1} \mathbf{K}^*(\mathbf{s}_n, s^*), \end{aligned}$$

and $\sigma^2 = \mathbb{V}[x(s^*)]$. Thus

$$\begin{aligned} \mathbb{P}(W < z) &= \mathbb{E}[\mathbb{P}(W < z | \mathbf{u}_n)] \\ &= \mathbb{E} \left[\Phi \left(\frac{z}{\sqrt{V(\mathbf{u}_n)}} \right) \right]. \end{aligned}$$

A.4 Proof of Theorem 3.4

First, our assumptions in the hypothesis imply that k is continuous everywhere in \mathbb{S}^2 except where $s_1 = s_2$. To see this, take any distinct $s_1, s_2 \in \mathbb{S}$ and sequence s_1^m, s_2^m converging to (s_1, s_2) . The sequence $c(s_1^m + u_1^m, s_2^m + u_2^m)$ is bounded and converges in distribution to $c(s_1 + u_1, s_2 + u_2)$. Thus, by the Dominated Convergence theorem, $k(s_1^m, s_2^m) \rightarrow k(s_1, s_2)$.

Now, for any $n \in \mathbb{N}$, the KILE MSE in predicting $x(s^*)$ given \mathbf{y}_n is

$$\begin{aligned} \mathbb{E}[(x(s^*) - \hat{x}_{\text{KILE}}(x^*))^2] &= \mathbb{V}[x(s^*)] - 2\mathbf{C}(s^*, \mathbf{s}_n)\mathbf{C}(\mathbf{s}_n, \mathbf{s}_n)^{-1}\mathbf{K}^*(\mathbf{s}_n, s^*) \\ (16) \quad &+ \mathbf{C}(s^*, \mathbf{s}_n)\mathbf{C}(\mathbf{s}_n, \mathbf{s}_n)^{-1}\mathbf{K}(\mathbf{s}_n, \mathbf{s}_n)\mathbf{C}(\mathbf{s}_n, \mathbf{s}_n)^{-1}\mathbf{C}(\mathbf{s}_n, s^*). \end{aligned}$$

The matrix $\mathbf{C}(\mathbf{s}_n, \mathbf{s}_n)$ is symmetric and positive definite, and thus it can be written as $\mathbf{C}(\mathbf{s}_n, \mathbf{s}_n) = \mathbf{Q}\mathbf{\Lambda}\mathbf{Q}'$, where \mathbf{Q} is an orthogonal matrix and $\mathbf{\Lambda}$ is diagonal. Assume without loss of generality the entries are $\mathbf{\Lambda}$ are ordered $0 < \lambda_1 < \dots < \lambda_n$. Similarly, write $\mathbf{K}(\mathbf{s}_n, \mathbf{s}_n) = \mathbf{R}\mathbf{\Omega}\mathbf{R}'$. Further letting $\mathbf{a} = \mathbf{C}(s^*, \mathbf{s}_n)\mathbf{Q}$, $\mathbf{b} = \mathbf{Q}'\mathbf{K}(\mathbf{s}_n, s^*)$, and $\mathbf{D} = \mathbf{Q}'\mathbf{R}\mathbf{\Omega}^{\frac{1}{2}}$, we can write (16) as

$$\begin{aligned} \mathbb{E}[(x(s^*) - \hat{x}_{\text{KILE}}(x^*))^2] &= \mathbb{V}[x(s^*)] - 2\mathbf{a}'\mathbf{\Lambda}^{-1}\mathbf{b} + \mathbf{a}'\mathbf{\Lambda}^{-1}\mathbf{D}\mathbf{D}'\mathbf{\Lambda}^{-1}\mathbf{a} \\ (17) \quad &= \mathbb{V}[x(s^*)] - 2\sum_{i=1}^n \frac{a_i b_i}{\lambda_i} + \sum_{j=1}^n \left(\sum_{i=1}^n \frac{a_i D_{ij}}{\lambda_i} \right)^2. \end{aligned}$$

Let $\xi = \lambda_1^{-1}$; then Equation (17) can be expressed as

$$(18) \quad \mathbb{E}[(x(s^*) - \hat{x}_{\text{KILE}}(x^*))^2] = \xi^2 \left(\sum_{j=1}^n a_1^2 D_{1j}^2 \right) + h(\xi),$$

where h is linear in ξ .

Without loss of generality, assume $s_1 \rightarrow s_2$. Thus $\mathbf{C}(\mathbf{s}_n, \mathbf{s}_n)$ becomes rank $n-1$, with $\lambda_1 \rightarrow 0$ and for all $i > 1$, $\lambda_i \rightarrow \lambda_i^* > 0$. Thus $\xi \rightarrow \infty$. However, $\mathbf{K}(\mathbf{s}_n, \mathbf{s}_n)$ does not become singular, since $\mathbb{P}(u_1 \neq u_2) < 1$ implies

$$\lim_{s_1 \rightarrow s_2} k(s_1, s_2) \neq \mathbb{V}[y(s_2)].$$

Since k is continuous and $\mathbf{K}(\mathbf{s}_n, \mathbf{s}_n)$ nonsingular in the limit, all of the terms besides ξ in (17) converge as $s_1 \rightarrow s_2$; that is $\mathbf{a} \rightarrow \mathbf{a}^*$, $\mathbf{b} \rightarrow \mathbf{b}^*$, and $\mathbf{D} \rightarrow \mathbf{D}^*$ as $s_1 \rightarrow s_2$. Moreover, we cannot have $D_{1j}^* = 0$ for all j , as this contradicts $\mathbf{K}(\mathbf{s}_n, \mathbf{s}_n)$ remaining full-rank. Lastly, since $\mathbf{C}(s^*, \mathbf{s}_n) \neq \mathbf{0}$ and \mathbf{Q} is orthogonal, $a_i \neq 0$ and $a_i^* \neq 0$ for all $i = 1, \dots, n$.

Thus the quadratic coefficient in (18), $\sum_{j=1}^n a_1^2 D_{1j}^2$ is strictly positive, and $h(\xi) = \mathcal{O}(\xi)$. Because $\xi \rightarrow \infty$, we get

$$\lim_{s_1 \rightarrow s_2} \mathbb{E}[(x(s^*) - \hat{x}_{\text{KILE}}(x^*))^2] = \infty.$$

For pathological choices of $g_{\mathbf{s}_n}$ where k is not continuous everywhere and limits for \mathbf{b} and \mathbf{D} may not exist, all components of these terms can be still be bounded, which is sufficient for Theorem 3.4 to hold.

A.5 Proof of Proposition 4.1

Bayes rule predictors by definition satisfy $R_\pi(\pi) \leq R_\pi(\tilde{\pi})$, which confirms the two inequalities in the statement of Proposition 4.1. The equality $R_\pi(\pi_0) = R_{\pi_0}(\pi_0)$ holds since the risk of the Bayes estimator under π_0 is a quadratic form, and therefore constant for all $\pi \in \Pi_{0,\mathbf{C}}$:

$$\begin{aligned} R_{\pi_0}(\pi_0) &= \mathbb{E}_\pi[(\mathbb{E}_{\pi_0}[x(s^*)|\mathbf{x}_n] - x(s^*))^2] \\ &= \mathbb{E}_\pi[(\mathbf{C}(s^*, \mathbf{s}_n)\mathbf{C}(\mathbf{s}_n, \mathbf{s}_n)^{-1}\mathbf{x}_n - x(s^*))^2] \\ &= c(s^*, s^*) - \mathbf{C}(s^*, \mathbf{s}_n)\mathbf{C}(\mathbf{s}_n, \mathbf{s}_n)^{-1}\mathbf{C}(\mathbf{s}_n, s^*) \\ &= R_\pi(\pi_0). \end{aligned}$$

ACKNOWLEDGEMENTS

We thank Luke Bornn and Peter Huybers for helpful comments and encouragement. NSP was partially supported by an ONR grant. DC was partially supported by a research grant from the Harvard University Center for the Environment.

REFERENCES

- BANERJEE, S., CARLIN, B. P. and GELFAND, A. E. (2014). *Hierarchical modeling and analysis for spatial data*. Crc Press.
- BANERJEE, S., GELFAND, A. E., FINLEY, A. O. and SANG, H. (2008). Gaussian predictive process models for large spatial data sets. *Journal of the Royal Statistical Society: Series B (Statistical Methodology)* **70** 825–848.
- BARBER, J. J., GELFAND, A. E. and SILANDER, J. A. (2006). Modelling map positional error to infer true feature location. *Canadian Journal of Statistics* **34** 659–676.
- BONNER, M. R., HAN, D., NIE, J., ROGERSON, P., VENA, J. E. and FREUDENHEIM, J. L. (2003). Positional accuracy of geocoded addresses in epidemiologic research. *Epidemiology* **14** 408–412.
- BROHAN, P., KENNEDY, J. J., HARRIS, I., TETT, S. F. and JONES, P. D. (2006). Uncertainty estimates in regional and global observed temperature changes: A new data set from 1850. *Journal of Geophysical Research: Atmospheres (1984–2012)* **111**.
- CARROLL, R. J., RUPPERT, D., STEFANSKI, L. A. and CRAINICEANU, C. M. (2006). *Measurement error in nonlinear models: a modern perspective*. CRC press.
- COWTAN, K. and WAY, R. G. (2014). Coverage bias in the HadCRUT4 temperature series and its impact on recent temperature trends. *Quarterly Journal of the Royal Meteorological Society* **140** 1935–1944.
- CRESSIE, N. A. and CASSIE, N. A. (1993). *Statistics for spatial data* **900**. Wiley New York.
- CRESSIE, N. and JOHANNESSON, G. (2008). Fixed rank kriging for very large spatial data sets. *Journal of the Royal Statistical Society: Series B (Statistical Methodology)* **70** 209–226.
- CRESSIE, N. and KORNAK, J. (2003). Spatial statistics in the presence of location error with an application to remote sensing of the environment. *Statistical science* **18** 436–456.
- DIRECTOR, H. and BORNN, L. (2015). Connecting Point-Level and Gridded Moments in the Analysis of Climate Data. *Journal of Climate*.
- FANSHAWE, T. and DIGGLE, P. (2011). Spatial prediction in the presence of positional error. *Environmetrics* **22** 109–122.
- FERGUSON, T. S. (1996). *A course in large sample theory* **49**. Chapman & Hall London.
- GABROSEK, J. and CRESSIE, N. (2002). The effect on attribute prediction of location uncertainty in spatial data. *Geographical Analysis* **34** 262–285.
- GELMAN, A. and SHIRLEY, K. (2011). Inference from simulations and monitoring convergence. *Handbook of Markov chain Monte Carlo* 163–174.
- GELMAN, A., CARLIN, J. B., STERN, H. S., DUNSON, D. B., VEHTARI, A. and RUBIN, D. B. (2014). *Bayesian data analysis, Third Edition*. Chapman & Hall.
- GUYON, X. (1982). Parameter estimation for a stationary process on a d-dimensional lattice. *Biometrika* **69** 95–105.

- HEYDE, C. C. (1997). *Quasi-likelihood and its application: a general approach to optimal parameter estimation*. Springer Science & Business Media.
- HOMAN, M. D. and GELMAN, A. (2014). The no-U-turn sampler: Adaptively setting path lengths in Hamiltonian Monte Carlo. *The Journal of Machine Learning Research* **15** 1593–1623.
- JONES, P., LISTER, D., OSBORN, T., HARPHAM, C., SALMON, M. and MORICE, C. (2012). Hemispheric and large-scale land-surface air temperature variations: An extensive revision and an update to 2010. *Journal of Geophysical Research: Atmospheres (1984–2012)* **117**.
- LAN, S., STREETS, J. and SHAHBABA, B. (2013). Wormhole Hamiltonian Monte Carlo. *arXiv preprint arXiv:1306.0063*.
- LAWSON, A. B. (1994). Using spatial Gaussian priors to model heterogeneity in environmental epidemiology. *The Statistician* 69–76.
- LINDGREN, F., RUE, H. and LINDSTRÖM, J. (2011). An explicit link between Gaussian fields and Gaussian Markov random fields: the stochastic partial differential equation approach. *Journal of the Royal Statistical Society: Series B (Statistical Methodology)* **73** 423–498.
- MANN, M. E., ZHANG, Z., HUGHES, M. K., BRADLEY, R. S., MILLER, S. K., RUTHERFORD, S. and NI, F. (2008). Proxy-based reconstructions of hemispheric and global surface temperature variations over the past two millennia. *Proceedings of the National Academy of Sciences* **105** 13252–13257.
- MARDIA, K. V. and GOODALL, C. R. (1993). Spatial-temporal analysis of multivariate environmental monitoring data. *Multivariate environmental statistics* **6** 76.
- MATHERON, G. (1962). *Traité de géostatistique appliquée*. Editions Technip.
- MENG, X.-L. (1994). Multiple-imputation inferences with uncongenial sources of input. *Statistical Science* 538–558.
- MENG, X.-L. and XIE, X. (2014). I got more data, my model is more refined, but my estimator is getting worse! Am I just dumb? *Econometric Reviews* **33** 218–250.
- MORICE, C. P., KENNEDY, J. J., RAYNER, N. A. and JONES, P. D. (2012). Quantifying uncertainties in global and regional temperature change using an ensemble of observational estimates: The HadCRUT4 data set. *Journal of Geophysical Research: Atmospheres (1984–2012)* **117**.
- MORRIS, C. N. (1983). Natural exponential families with quadratic variance functions: statistical theory. *The Annals of Statistics* 515–529.
- NEAL, R. M. (2005). Hamiltonian importance sampling. Talk presented at the Banff International Research Station (BIRS) workshop on Mathematical Issues in Molecular Dynamics, June 2005.
- NEAL, R. M. (2011). MCMC using Hamiltonian dynamics. *Handbook of Markov Chain Monte Carlo* **2**.
- QIN, Z. S. and LIU, J. S. (2001). Multipoint Metropolis method with application to hybrid Monte Carlo. *Journal of Computational Physics* **172** 827–840.
- RASMUSSEN, C. E. (2006). Gaussian processes for machine learning.
- RICHARD, A. et al. (2012). A new estimate of the average earth surface land temperature spanning 1753 to 2011. *Geoinformatics & Geostatistics: An Overview*.
- ROBERTS, G. O., ROSENTHAL, J. S. et al. (2001). Optimal scaling for various Metropolis-Hastings algorithms. *Statistical science* **16** 351–367.
- SACKS, J., WELCH, W. J., MITCHELL, T. J. and WYNN, H. P. (1989). Design and analysis of computer experiments. *Statistical science* 409–423.
- SALAZAR, R. and TORAL, R. (1997). Simulated annealing using hybrid Monte Carlo. *Journal of Statistical physics* **89** 1047–1060.
- SMITH, R. L. (2004). Asymptotic theory for kriging with estimated parameters and its application to network design.
- SRINIVAS, N., KRAUSE, A., KAKADE, S. M. and SEEGER, M. (2009). Gaussian process optimization in the bandit setting: No regret and experimental design. *arXiv preprint arXiv:0912.3995*.
- STEIN, M. L. (1999). *Interpolation of spatial data: some theory for kriging*. Springer Science & Business Media.
- STEIN, M. L., CHI, Z. and WELTY, L. J. (2004). Approximating likelihoods for large spatial data sets. *Journal of the Royal Statistical Society: Series B (Statistical Methodology)* **66** 275–296.
- STAN DEVELOPMENT TEAM (2014). RStan: the R interface to Stan, Version 2.5.0.
- TINGLEY, M. P. (2012). A Bayesian ANOVA scheme for calculating climate anomalies, with applications to the instrumental temperature record. *Journal of Climate* **25** 777–791.

- TINGLEY, M. P. and HUYBERS, P. (2010). A Bayesian algorithm for reconstructing climate anomalies in space and time. Part I: Development and applications to paleoclimate reconstruction problems. *Journal of Climate* **23** 2759–2781.
- VARIN, C., REID, N. M. and FIRTH, D. (2011). An overview of composite likelihood methods. *Statistica Sinica* **21** 5–42.
- VEREGIN, H. (1999). Data quality parameters. *Geographical information systems* **1** 177–189.
- WARD, M. H., NUCKOLS, J. R., GIGLIERANO, J., BONNER, M. R., WOLTER, C., AIROLA, M., MIX, W., COLT, J. S. and HARTGE, P. (2005). Positional accuracy of two methods of geocoding. *Epidemiology* **16** 542–547.
- WARNES, J. and RIPLEY, B. (1987). Problems with likelihood estimation of covariance functions of spatial Gaussian processes. *Biometrika* **74** 640–642.
- ZHU, Z. and STEIN, M. L. (2006). Spatial sampling design for prediction with estimated parameters. *Journal of Agricultural, Biological, and Environmental Statistics* **11** 24–44.
- ZIMMERMAN, D. L. and CRESSIE, N. (1992). Mean squared prediction error in the spatial linear model with estimated covariance parameters. *Annals of the institute of statistical mathematics* **44** 27–43.
- ZIMMERMAN, D. L., LI, J. and FANG, X. (2010). Spatial autocorrelation among automated geocoding errors and its effects on testing for disease clustering. *Statistics in medicine* **29** 1025–1036.
- ZIMMERMAN, D. L. and SUN, P. (2006). Estimating spatial intensity and variation in risk from locations subject to geocoding errors. *Iowa City: University of Iowa*.